CHEMISTRY
A EUROPEAN JOURNAL

DOI: 10.1002/chem.201001051

Proaromaticity: Organic Charge-Transfer Chromophores with Small HOMO–LUMO Gaps

Yi-Lin Wu,[a] Filip Bureš,[b] Peter D. Jarowski,[a] W. Bernd Schweizer,[a] Corinne Boudon,[c] Jean-Paul Gisselbrecht,[c] and François Diederich*[a]

Abstract: Novel donor- and/or acceptor-substituted cross-conjugated carbocycles based on quinoids or expanded quinoids, with radiaannulene perimeters, were prepared and investigated to validate proaromaticity as a concept for reducing HOMO–LUMO gaps in push–pull chromophores. Analyses of IR, ^{1}H NMR, and UV/Vis/NIR spectra in conjunction with molecular structures determined by X-ray diffraction show that these push–pull quinoids have significant charge-separated ground states. This feature results in small optical gaps (near IR region) and diatropic magnetic environments inside the carbocycles, as suggested by nucleus-independent chemical shift (NICS) calculations. The NICS results, together with the bond-length analysis of the quinoid spacers, provide strong support that proaromaticity, that is, aromatized zwitterionic mesomeric contributions in the ground state, is effective. A push–pull tetrakis(ethynediyl)-expanded quinoid chromophore represents the first proaromatic radiaannulene.

Keywords: annulenes · aromaticity · computational chemistry · conjugation · donor–acceptor systems

Introduction

Small band-gap organic chromophores have found applications in near infrared (NIR) fluorophores,[1] NIR photodetectors/photovoltaics,[2] and nonlinear optical (NLO) materials.[3] These NIR organic materials are conventionally produced and examined in the realm of π-conjugated polymers; studies have revealed that the small band-gap could be achieved by 1) increasing the conjugation length, 2) attaching powerful electron donors (D) and acceptors (A), and 3) reducing the bond-length alternation (BLA) of the conjugated backbones.[4] The first two approaches 1) and 2) are also popularly investigated by many research groups to tailor the optoelectronic properties of monomeric chromophores, denoted D-π-A systems. We reported in the past years on families of nonplanar π-conjugated intramolecular charge-transfer (ICT) chromophores featuring potent polycyano acceptors and a variety of donors, which find application in optoelectronic devices.[5]

The third approach of varying BLA, on the other hand, is based on the fact that the extent of π-electron delocalization in polyene-type polymers is limited by Peierls distortion of the polymer backbones that results in finite energy separations between the valence molecular orbitals. In polyarenes, π-electron delocalization is confined within the aromatic units, as polarization through the aromatic ring meets resistance due to the partial loss of aromaticity. Increasing the double-bond character of the σ-bond linkage between arenes (or the quinoid character of the arene units) would, in turn, reduce the BLA of the whole polymer system, facilitate electron delocalization, and therefore reduce the HOMO–LUMO gap. This is the case in polyisothianaphthene (PITN) and polyindenofluorene (PIF), for which NIR electronic absorptions of about 1.2–1.5 eV have been reported.[6]

The HOMO–LUMO gaps in monomeric chromophores are also influenced by the BLA of the π spacers, as the electronic structures are immediate functions of molecular geometries. In addition to the effect on electronic gap, Marder

[a] Y.-L. Wu, Dr. P. D. Jarowski, Dr. W. B. Schweizer, Prof. Dr. F. Diederich
Laboratorium für Organische Chemie
ETH-Zürich, Hönggerberg, HCI, 8093 Zürich (Switzerland)
Fax: (+41) 44.632.1109
E-mail: diederich@org.chem.ethz.ch

[b] Prof. Dr. F. Bureš
Institute of Organic Chemistry and Technology
Faculty of Chemical Technology, University of Pardubice
Studentská 573, Pardubice, 532 10 (Czech Republic)

[c] Prof. Dr. C. Boudon, Dr. J.-P. Gisselbrecht
Laboratoire d'Electrochimie et de Chimie Physique du Corps Solide
UMR 7177 C.N.R.S, Université de Strasbourg
4, rue Blaise Pascal, 67000 Strasbourg (France)

Supporting information for this article is available on the WWW under http://dx.doi.org/10.1002/chem.201001051.

et al. reported the interrelationship between molecular hyperpolarizabilities (β and γ) and BLAs of oligomethines and oligoenes in the 1990s.[7] Despite the fact that the fundamentals of oligoene-based systems are better understood, organic materials that have been explored for applications are mostly based on aromatic structural motifs for their intrinsic superior stability; benzenoids in particular. Less aromatic arenes, such as thiophenes, which pay smaller energetic penalties of de-aromatization upon polarization, are frequently used for organic optoelectronics. Conceptually, replacing arenes by quinoid spacers would make polarization or CT excitation even more favorable.

The highly colored compound **1** was published by Gompper et al. in the late 1960s as the first example of D-A chromophores with a quinoid spacer (abbreviated as D-Q-A afterwards).[8] Over the past few decades, a similar design principle has only been sparsely applied, incorporating naphthoquinoid, anthraquinoid, or heteroquinoid π spacers in some cases.[9] The intense, low-energy absorptions of these quinoid chromophores were proposed to result from the aromatized zwitterionic mesomeric contribution in the ground state—the term "proaromatization" was thus coined. The comparable degrees of charge separation in the electronic ground state and in the ICT excited state reduce the energy that is needed for excitation. Large, negative solvatochromism and negative first molecular hyperpolarizabilities have been observed for systems such as **2** and **3**, implying significant zwitterionic character in the ground states.[9a,b] CT chromophores with proaromatic donors or acceptors in recent years have found successful application as NLOphores and for molecular recognition purposes.[10]

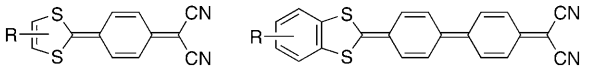

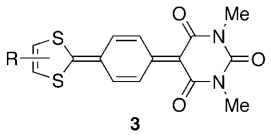

Based on the neutral and zwitterionic limits of canonical structures, the concept of proaromaticity seems to be extremely appealing; however, the fundamentals of proaromaticity have not been systematically studied. Since the efficient ground-state charge transfer might also originate from a mechanism that does not involve aromaticity, a validation of proaromaticity is clearly desirable.

In this article, we report the preparation of the push–pull quinoid systems **4–6** and related model systems and analyze their spectra and molecular structures. Among them, push–pull diphenoquinodimethane **5** is expected to be doubly proaromatic and the expanded quinoid **6** would be the first proaromatic radiaannulene macrocycle.[11] *N,N*-Dimethylanilino (DMA) or *N,N*-dibutylanilino (DBA) residues were used as electron donors, while cyano or *para*-nitrophenyl groups were employed as electron acceptors. Indeed, these molecules show low-energy absorption maxima at 600–850 nm, with the absorption edge down to 1200 nm (1.0 eV). Their electronic absorption, ^{1}H NMR, and IR spectra, and their bond-length alternation are compared to those of reference compounds lacking quinoid spacers to highlight the facile ground-state charge transfer in D-Q-A systems. Nucleus-independent chemical shifts (NICS) were calculated to analyze the aromatic characters in such quinoid systems, and a preliminary evaluation of aromatic stabilization energies (ASE) of proaromatic systems was performed within a set of hyperhomodesmotic reactions. Combining our results from bond-length analysis and NICS calculations, the aromaticity of push–pull quinoid molecules was demonstrated.

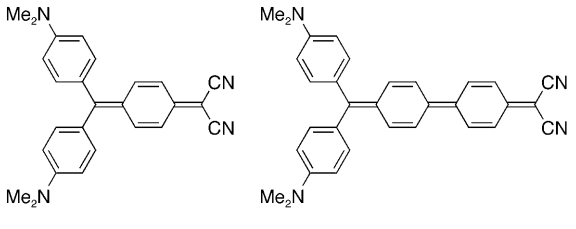

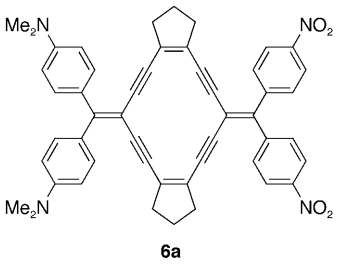

Results and Discussion

Synthesis: The reference cyclohexyl and cyclohexenyl compounds were published by our group,[12] and the synthesis is briefly summarized in Scheme 1. Reaction of the cyclohexyl compounds **7** and **8** with 2,3-dichloro-5,6-dicyano-1,4-benzoquinone (DDQ) resulted in partial oxidation to give the cyclohexenes **9** (50%) and **10** (43%), respectively. The quinoid linkages between the push/pull functionalities were synthesized form their aromatic parents through a dehydration reaction published for compound **4**[9d] to avoid decomposition or polymerization under oxidative conditions. Electron-

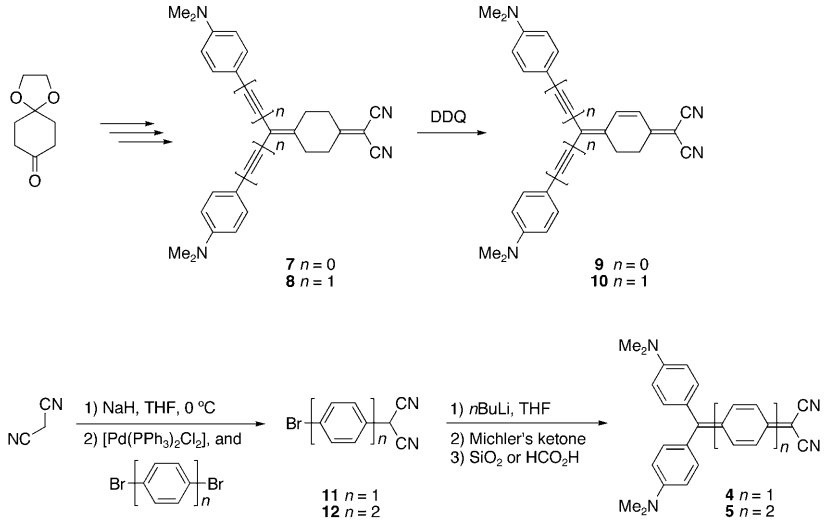

Scheme 1. Synthesis of push–pull quinoid chromophores **4** and **5**, and their reference compounds with cyclohex-1,4-diyl or cyclohex-2-en-1,4-diyl bridging units.

withdrawing, malononitrile-substituted phenyl **11** and biphenyl **12** were obtained by a Pd-catalyzed Takahashi reaction[13] with readily available *para*-dibromophenyl/biphenyl precursors. Addition of the corresponding dilithiated aryl anion to Michler's ketone, followed by dehydration, afforded the desired quinoids **4** and **5** in reasonable yields (88 and 51%, respectively, Scheme 1).

Preparation of the radialannulene-type expanded quinoid molecule **6** was achieved in a modular approach. The electron acceptor, electron donor, and the *cis*-hexa-3-en-1,5-diyn-1,6-diyl moieties were synthesized separately, and assembled at the later stages to construct the macrocycle (Scheme 2). The pre-formed *cis* geometry in the cyclopent-1-en-1,2-diyl moiety[14] was exploited not only to simplify the synthesis, but also to avoid the π-electron localization in the synthetically more accessible *ortho*-diethynylbenzene derivatives.

The acceptor unit **13** was obtained by dibromoolefination of bis(4-nitrophenyl)methanone[15] in 72% yield. For the donor part, Suzuki cross-coupling of *gem*-dibromo compound **14**[16] with 4-(dimethylamino)phenylboronic acid produced the triisopropylsilyl (TIPS) protected donor precursor

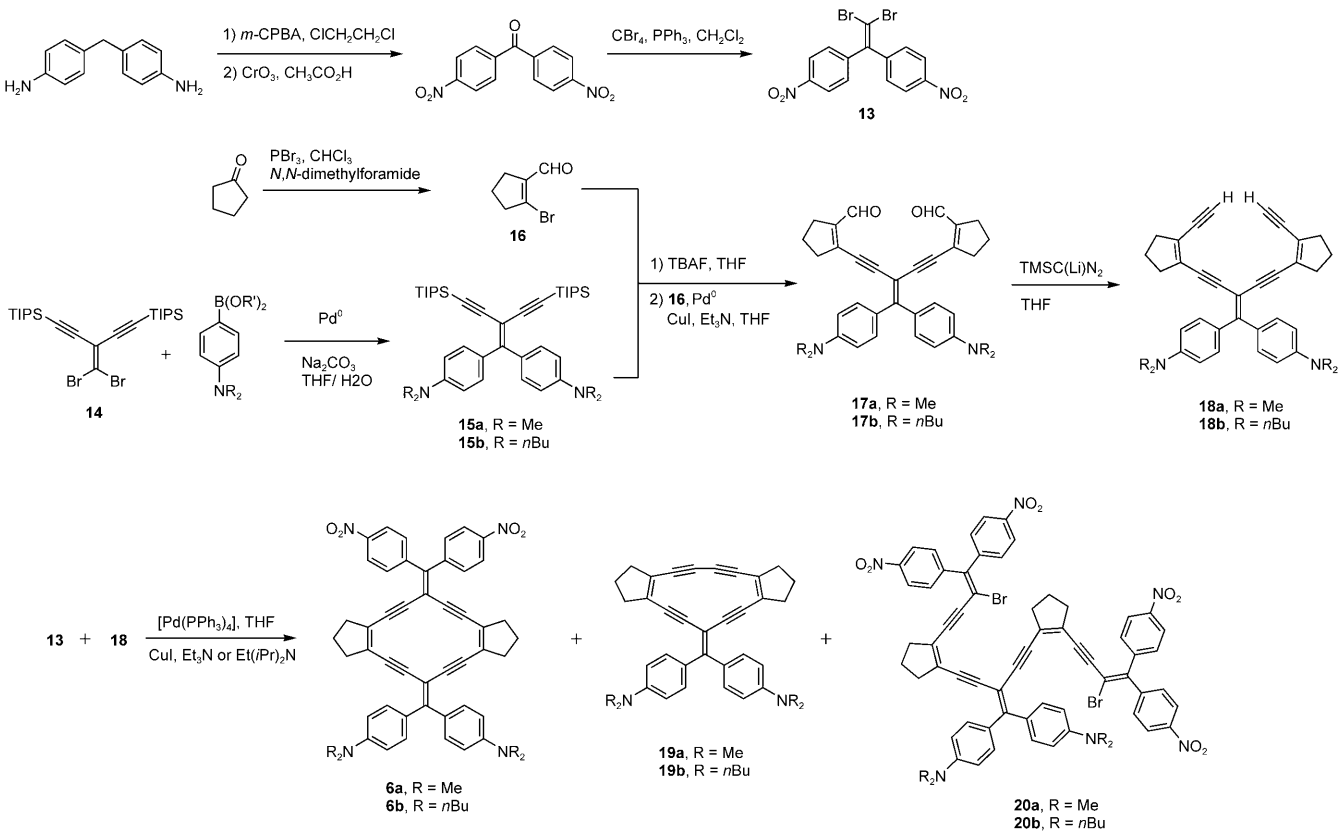

Scheme 2. Synthesis of push–pull chromophores **6**, **19**, and **20**. *m*-CPBA = *meta*-chloroperbenzoic acid. For the specific Pd catalyst used for **14**→**15** and **15**→**16**, please see the Experimental Section.

15a, which was then treated with tetrabutylammonium fluoride trihydrate (TBAF·3 H_2O) in tetrahydrofuran (THF) to remove the protecting group. Subsequently, Sonogashira reaction between desilylated **15a** and 2-bromocyclopent-1-enecarbaldehyde (**16**)[17] afforded biscarbaldehyde **17a**. One-step alkynylation of **17a** was achieved by treatment with lithiated trimethylsilyldiazomethane [TMSC(Li)N_2] to give diethynyl derivative **18a**.[18] Closure of the macrocyclic ring was realized by a double Sonogashira cross-coupling reaction between **13** and **18a**. Though low-yielding, the D-Q-A macrocycle **6a** was synthesized under oxygen-free conditions (41 %), whereas the molecule of homocoupling, **19a**, was found as the major product if traces of dioxygen were present; the 2:1 adduct **20a** between **13** and **18a** was occasionally also isolated in a small amount. The DBA-substituted macrocycle **6b** was prepared by a similar route (**14**→**15b**→**17b**→**18b**→**6b**) starting from the DBA–pinacol ester (19 % yield for the ring-closing step). The *n*-butyl substituents provide better solubility for both analysis and characterization.

IR and ^{1}H NMR spectra: Selected IR and ^{1}H NMR data of **4**–**6a**, **7**, **9**, **20a**, and other model compounds are listed in Table 1 to illustrate the extent of ground-state charge separation. Since the stretching frequency of the cyano groups is sensitive to the vicinal electron density, it is a good probe for the ground-state charge transfer. The bond strength and therefore the vibrational frequency of CN groups are reduced by the presence of increased vicinal electron density, which interacts with the π* orbital of the C≡N group. For reference, the stretching frequency, $\tilde{\nu}_{CN}=2178\ cm^{-1}$, for lithium dicyano(phenyl)methanide ($Li^+[C(CN)_2Ph]^-$) models a full formal vicinal negative charge, while the stretching frequency, $\tilde{\nu}_{CN}=2226\ cm^{-1}$, for TCNQ serves as a model without formal vicinal charge.[9a,d] The CN stretches at $\tilde{\nu}_{CN}=2230$ and 2212 cm^{-1} for compounds **7** and **9**, respectively, point to a small formal charge at the corresponding dicyanovinyl sites. On the other hand, the lower values for **4** ($\tilde{\nu}_{CN}=2183\ cm^{-1}$) and **5** ($\tilde{\nu}_{CN}=2168\ cm^{-1}$) imply considerable CT character in the ground state. The smaller $\tilde{\nu}_{CN}$ frequency for compound **5** might be due to the twofold aromatization gained from ICT; in contrast, for **4**, the gain of onefold aromatization stabilization is concomitantly compensated by the loss of aromaticity shared by the two aniline donors, making CT in **4** less energetically favored (Scheme 3).

Table 1. Selected IR and ^{1}H NMR data for **4**, **5**, **6a**, **7**, **9**, **19a**, **20a**, $Li^+[C(CN)_2Ph]^-$, and TCNQ.

	δ [ppm][a]	$\tilde{\nu}_{CN}$ [cm^{-1}]
$Li^+[C(CN)_2Ph]^-$	–	2178[b]
TCNQ	–	2226
7	2.95	2230
9	3.02, 6.55, 7.01	2212
4	3.16, 7.14, 7.17	2183
5	3.31, 6.87, 7.14, 7.23, 7.45	2168
19a	3.04	–
20a	2.99	–
6a	3.02	–

[a] Only the ^{1}H NMR chemical shifts ($CDCl_3$) of *N*,*N*-dimethylamino groups ($\delta\approx3$ ppm) and/or the olefinic protons ($\delta\approx6.5$–7.5 ppm) are shown. [b] $\tilde{\nu}_{CN}$ of the corresponding Na^+ salt is similar.

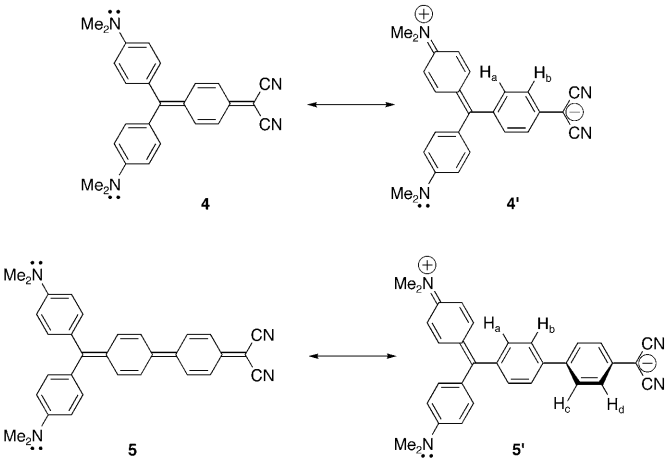

Scheme 3. Contribution of charge-transfer aromatization (proaromatization) to the ground state structures of **4** and **5**.

The extent of downfield shifts of the ^{1}H NMR resonance of the *N*,*N*-dimethylamino moieties corroborates the findings from CN vibration analysis. Additionally, **4** exhibits a narrow range of the AA′BB′ signals from H_a and H_b at 7.14 and 7.17 ppm. The appearance of these proton signals in the aromatic region, downfield from the olefinic region (compared to **9**), further supports the reduced quinoid character in the ground state, due to ICT aromatization. In the case of **5**, proton signals also appear in the aromatic region (6.87, 7.14, 7.23, and 7.45 ppm for $H_{a–d}$).

In the expanded systems **6** and **20**, there is no formally olefinic proton; however, the larger downfield shift of the *N*,*N*-dimethylamino protons in **6a** (3.02 ppm) suggests a greater extent of charge separation in the ground state, as compared to **20a** (2.99 ppm), which in fact has more *para*-nitrophenyl acceptor groups.

Electronic absorption spectra: UV/Vis/NIR spectra of **4**, **5**, **7**, and **9** are overlaid in Figure 1 to compare the effects of the π spacers bearing similar carbon skeletons. Compound **7** exhibits aniline-centered bands at $\lambda_{max}=280$ and 358 nm;[19] the non-conjugated and distant dicyanovinyl group has little influence on the absorption of the DMA ring. Conjugating the two electronically active push–pull moieties by one double-bond results in an ICT absorption at $\lambda_{max}=528$ nm (compound **9**). Installation of another double bond into the cyclohexyl ring creates an even lower-energy band at $\lambda_{max}=$ 698 nm with an energy gap of 1.55 eV estimated from the absorption on-set in CH_2Cl_2 (compound **4**). This striking difference in absorption spectra of **4** and **9** cannot be simply explained by the difference of the electron donor/acceptor nor the conjugation length, since identical donor/acceptor groups are used, and identical linear conjugation paths are

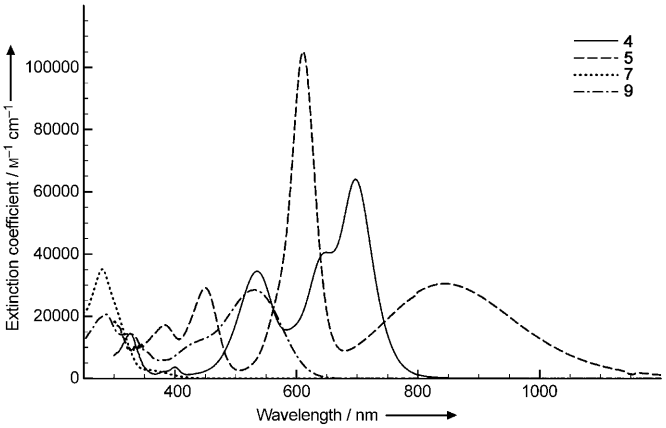

Figure 1. UV/Vis/NIR absorption spectra of compounds **4**, **5**, **7**, and **9** in CH_2Cl_2 at 298 K, $c \approx 10^{-5}$ M.

present in both molecules (the directions of the transition moments[20] for **4** and **9** are also similar; see illustration in the Supporting Information). Extending the conjugation pathway by an additional quinodimethane ring gives two major absorptions (compound **5**): one is located in the visible region with $\lambda_{max} = 610$ nm (estimated energy gap = 1.53 eV), and the other broad absorption is located in the NIR region with $\lambda_{max} = 845$ nm (absorption edge ≈ 1200 nm; 1.03 eV). These lowest energy absorptions ($\lambda_{max} = 698$ nm for **4**, $\lambda_{max} = 845$ nm for **5**, and $\lambda_{max} = 528$ nm for **9**) could be quenched by the addition of trifluoroacetic acid.

The interesting behavior of the cross-conjugated cyclic π spacers is further disclosed by comparing the series of ethynediyl-expanded molecules (Figure 2). The weakly strained

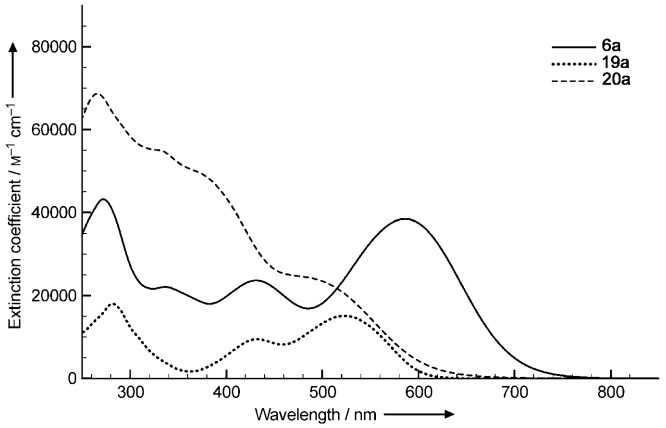

Figure 2. UV/Vis/NIR absorption spectra of compounds **6a**, **19a**, and **20a** in CH_2Cl_2 at 298 K, $c \approx 10^{-5}$ M.

(see below) macrocyclic C_{sp}/C_{sp^2} system acts as an electron acceptor in molecule **19a**, resulting in an ICT absorption at $\lambda_{max} = 540$ nm. Compound **20a** exhibits an absorption band around 500 nm; however, comparing this molecule to **19a**, the two compounds exhibit different extinction profiles, because of four *para*-nitrophenyl acceptors in compound **20a**. In view of the position of ICT bands, the accepting power of the four *para*-nitrophenyl groups through the enediyne spacers in **20a** seems to be similar to that of the weakly strained radiaannulenic cycle in **19a**. As in the cases of quinoids **4** and **5**, when the macrocycle is closed in compound **6a**, a lower energy absorption was found at $\lambda_{max} = 586$ nm (estimated energy gap = 1.62 eV). This decrease in CT transition energy cannot be attributed to the superior electron-accepting power of the two *para*-nitrophenyl groups present, since the number of accepting units here is in fact less then that of **20a**.

The absorption maxima of the lowest energy bands for **4**, **5**, and **6b** exhibit various degrees of negative solvatochromism. This implies strong charge-separation in their ground states which become more stabilized by increasing solvent polarity compared to the excited states. For example, λ_{max} of **4** shifts from 705 nm in THF, to 695 nm in acetone, and to 688 nm in EtOH ($\Delta E = 372$ cm^{-1} or 0.05 eV). For **6b**, λ_{max} appears at 622 nm in $CHCl_3$, at 596 nm in acetone, and at 589 nm in EtOH ($\Delta E = 901$ cm^{-1} or 0.11 eV). The largest negative solvatochromism was found for diphenoquinodimethane **5**: λ_{max} shifts from 1005 nm in THF, to 802 nm in acetone, and to 745 nm in MeCN ($\Delta E = 3473$ cm^{-1} or 0.43 eV), slightly more significant then reported for compound **2**.[9b] One should notice that the solvatochromism observed for **6b** with its large π system is also partly explainable by the changes in solvent polarizability. Plots of absorption maxima of the lowest energy bands against the Dimroth–Reichardt solvent polarity parameter E_T^N[21a] for **4**, **5**, and **6b**, and a plot against the Catalán–Hopf SP parameter[21b] for **6b** can be found in the Supporting Information.

Electrochemistry: Cyclic voltammetry (CV) and rotating-disk voltammetry (RDV) of **4**, **5**, **6a**, **6b**, **19a**, and **20a** were carried out in CH_2Cl_2 containing 0.1 M nBu$_4$NPF$_6$ as supporting electrolyte. Potentials reported in Table 2 are referenced to the ferricinium/ferrocene couple (Fc^+/Fc). For most of the species under investigation, due to electrode inhibition during redox processes, reproducible data could only be observed on freshly polished working electrodes (glassy carbon disk, 3 mm in diameter).

Species **4** gave a well-resolved voltammogram in contrast to **5**, for which the CVs are not well resolved due to adsorptions and inhibitions. For **4**, two re-oxidation potentials corresponding to the electrogenerated species from the second reduction steps were found at about −0.3 and +0.4 V by CV. If the scan is reversed after the first reduction, these signals are not observed. Comparison of the first oxidation and reduction potentials of **4** with those of **9** reflects that the decrease in optical HOMO–LUMO gap was mainly due to the substantial effect of the proaromatic spacer on both HOMO and LUMO levels. The first oxidation potential ($E_{1/2}$) changes from +0.33 V (**9**) to +0.17 V (**4**), whereas the first reduction potential shifts from −1.45 V (**9**) to −1.30 V (**4**).[12] The first oxidation was even shifted to −0.18 V for diphenoquinodimethane **5**.

Table 2. Cyclic voltammetry (CV; scan rate $\nu = 0.1\,V\,s^{-1}$) and rotating disk voltammetry (RDV) data for compounds **4**–**6**, **9**, **19a**, and **20a** in CH_2Cl_2 (+0.1 M nBu_4NPF_6).[a]

	CV			RDV	
	$E°$ [V][b]	ΔE_p [mV][c]	E_p [V][d]	$E_{1/2}$ [V][e]	Slope [mV][f]
4	+0.76	70		+0.75 (1e$^-$)	60
			+0.18	+0.17 (1e$^-$)	60
	−1.32	70		−1.30 (1e$^-$)	75
			−2.14	−2.16 (1e$^-$)	90
5	+0.75	60		+0.65	60
			−0.16	−0.18	60
	−1.08	70		−1.09	60
			−1.99	−1.97	
6a			+0.85	+0.90 (1e$^-$)	100
			+0.60	+0.60 (1e$^-$)	100
			+0.20	+0.16 (1e$^-$)	60
	−1.38	80		−1.38 (1e$^-$)	80
	−1.51	80		−1.54 (1e$^-$)	70
	−1.67	80		−1.70 (1e$^-$)	90
			−2.19		
6b	+0.79	70		+0.78 (1e$^-$)	60
	+0.54	70		+0.53 (1e$^-$)	60
	+0.10	60		+0.10 (1e$^-$)	70
	−1.38	70		−1.39 (1e$^-$)	70
	−1.54	70		−1.54 (1e$^-$)	70
	−1.71	60		−1.71 (1e$^-$)	70
			−2.23		
9	+0.70	80			
			+0.32	+0.33	50
			−1.71[g]	−1.45	
19a			+0.79	+0.63 (1e$^-$)	60
			+0.24	+0.26[h]	
	−1.87	90		−1.92 (1e$^-$)	60
			−2.34	−2.39 (1e$^-$)	70
20a			+0.77	+0.77 (1e$^-$)	120
			+0.57	+0.57 (1e$^-$)	125
	+0.23	75		+0.25 (1e$^-$)	100
	−1.41	100		−1.62[i]	
	−1.55	100			
			−2.05		
			−2.40		

[a] All potentials are given versus the Fc^+/Fc couple used as internal standard. [b] $E° = (E_{pc} + E_{pa})/2$, in which E_{pc} and E_{pa} correspond to the cathodic and anodic peak potentials, respectively. [c] $\Delta E_p = E_{pa} - E_{pc}$. [d] E_p = Irreversible peak potential. [e] $E_{1/2}$ = Half-wave potential. [f] Logarithmic analysis of the wave obtained by plotting E versus $\mathrm{Log}[I/(I_{lim} - I)]$. [g] Reversible when $\nu > 2\,V\,s^{-1}$. [h] Very low amplitude signal. [i] Large amplitude unresolved wave.

Analyzing the frontier molecular orbitals of **4**, **5**, and **9** gave some qualitative insight into the unusual redox behavior and hence the small optical gaps of **4** and **5** (Supporting Information). While the HOMO of **9** has significant coefficients on the DMA moieties, as one would expect, the HOMO of **4** is much more concentrated on the quinoid spacer and shifted closer toward the dicyanovinyl moiety; this observation is in line with what was seen in the IR study. A similar yet more noticeable HOMO distribution can be found for **5**. Thus, the oxidative potential might no longer be simply attributable to the anilino "donor" units.

Macrocyclic compounds **6a** and **6b** showed similar redox behavior by CV if one accepts the fact that for **6a**, none of the oxidation process was reversible in contrast to **6b**. Only at scan rates higher than $1\,V\,s^{-1}$, do these processes became reversible. The irreversible behavior may result from electrode inhibition or low solubility of the oxidized species. Studies by RDV gave, for both species, well-resolved waves of equal amplitude with no electrode inhibition. Macrocycle **19a** gave by CV, on reduction, a reversible one-electron transfer followed by an irreversible reduction. On oxidation, the first oxidation step was irreversible at all scan rates (up to $10\,V\,s^{-1}$), whereas the second oxidation was reversible but of small amplitude due to possible electrode inhibition. It had been previously shown that the ring system of radiaannulenes comprised of buta-1,3-diynediyl units is reducible at rather low potentials.[11b] In the present study, compound **19a** is reduced at −1.87 V, which is more negative and may be due to a lower number of conjugated double and triple bonds. Open-chain molecule **20a** gave several reduction and oxidation steps, which all seem to be irreversible. However, scanning over a potential range including only the first two reductions and the first oxidation shows that the electron transfers were reversible at all scan rates. From the peak amplitude, it turns out that the oxidation involves one electron, whereas the two reductions each involve two electrons, indicative of the reduction of the four nitrophenyl moieties.[22]

The effect of the expanded quinoid ring structure in **6a** to reduce the HOMO–LUMO gap was elucidated by comparing the electrochemical potentials to those of **20a**. The first oxidation potential ($E_{1/2}$) at +0.16 V for **6a** is smaller than that for **20a** (+0.25 V), and the first reduction potential ($E°$) at −1.38 V is also lower than that for **20a** (−1.41 V). All together, both the decrease in LUMO energies and the increase in HOMO energies account for the small optical/electrochemical gaps of push–pull proaromatic molecules, as clearly suggested by the electrochemical data for **4**–**6**.

Structural properties: The molecular structures **6b**, **19a**, and **20a** were analyzed by single-crystal X-ray diffraction (Figure 3). The crystal structures of **9** and **10** have been previously reported.[12] For comparisons, we use the X-ray data of **10**, for which a much better structure refinement value had been obtained. Also, the two compounds **9** and **10** behave similarly in absorption spectra and electrochemistry. Crystals of **4** and **5** with sufficiently good quality were unavailable. Thus, their computational gas-phase structures were optimized with Gaussian 09 at the level of B3LYP/6-31G(d) and used in place of experimental data. Solvated structures in MeCN were also calculated using the polarizable continuum model (PCM).[23]

Bond-length alternation (BLA, δr) for a 1,4-disubstituted hexagon can be numerically defined as depicted in Table 3, and this value is frequently used as a measure of how much the structure differs from perfectly delocalized benzene by

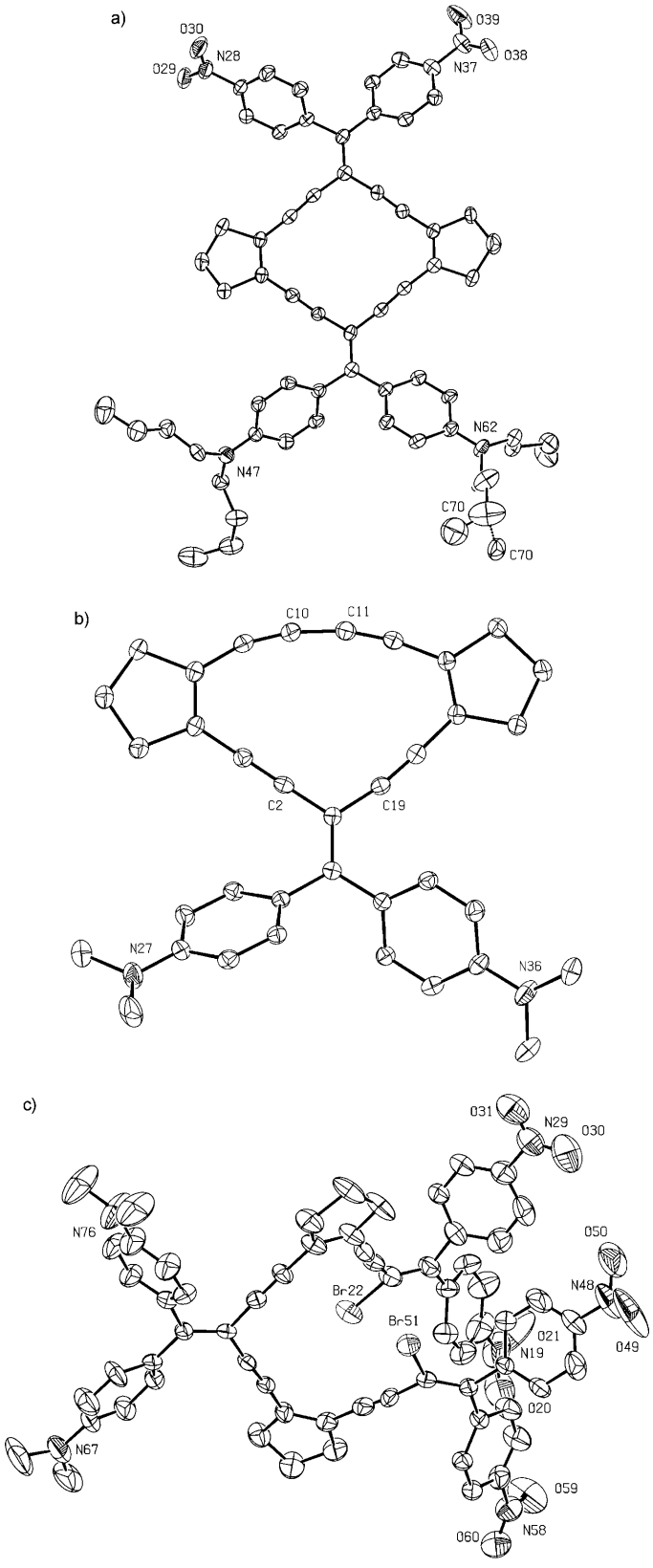

Figure 3. ORTEP plots of a) the expanded quinoid macrocycle **6b** (at 173 K, the bond to disordered C70 is drawn with a dashed line), b) DMA-substituted radiaannulene **19a** (123 K), and c) open-chain molecule **20a** (223 K). The thermal ellipsoids were shown at the 50% probability level. Heteroatoms and some carbon atoms are labeled with arbitrary numbering. Hydrogens and crystal solvents ($CDCl_3$ for **6b** and THF for **19a**) were removed for clarity.

Table 3. Bond-length alternation (BLA) for push–pull quinoids **4** and **5**, tetrakis(ethynediyl)-expanded quinoid **6b**, and their reference compounds **10**, **19a**, and **20a**; standard uncertainties are given in parenthesis.

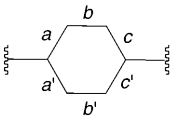

$$\delta r = \frac{[(a+c-2b)+(a'+c'-2b')]}{4}$$

	BLA (δr) [Å]	
	Aniline	Formal quinoid
4[a]	0.031 (vacuum) 0.043 (MeCN)	0.075 (vacuum) 0.053 (MeCN)
5[a]	0.033 (vacuum) 0.049 (MeCN)	0.060, 0.062 (vacuum) 0.032, 0.033 (MeCN)
10	0.013 (3), 0.015 (4)	–
6b	0.032 (6), 0.037 (6)	–
20a	0.027 (12), −0.001 (12)	–
19a	0.021 (3), 0.016 (3)	–

[a] Computational structures in either the gas-phase or solvated in MeCN with PCM model at the level of B3LYP/6-31G(d).

the effect of substituents.[24] The δr value is zero for benzene and 0.08–0.12 Å for fully quinoid systems, for instance, $\delta r =$ 0.08–0.10 Å for TCNQ. Since *N*,*N*-dialkylanilino groups were used as the electron donors in all the molecules under study, the BLA of the aniline rings can serve as a general probe for the degree of charge transfer in the ground state. For the cyclohex-2-en-1,4-diyl-bridged compound **10**, $\delta r =$ 0.014 (4) Å (average value for the two DMA rings) was found in its solid-state structure, showing only a small degree of charge transfer.[12] Much higher δr values of 0.031 (0.043 in MeCN with PCM model) and 0.033 Å (0.049 in MeCN) were found for the DMAs in push–pull quinoids **4** and **5**, respectively. The ethynediyl-expanded molecules present small δr values of 0.019 (3) Å for the DMA donors of **19a**, and 0.013 (12) Å for those of the open-chain compound **20a** (or 0.027 (12) for the ring with N67, since δr for the other aniline ring is chemically unreasonable); again, a much larger δr value of 0.035 (6) Å was observed for the DMAs of quinoid radiaannulene **6b**. Taken together, these data demonstrate the significance of the degree of charge transfer in the case of push–pull quinoid system, in addition to the data from the IR and ^{1}H NMR analysis.

Analyzing the bond-length pattern of the quinoid π spacers in **4** and **5** and the twisting between the two quinoid rings in **5** gave structural hints of proaromaticity. As shown in Table 3, $\delta r = 0.075$ and 0.061 Å were found for the formally quinoid rings of **4** and **5**, respectively, based on the computed structures in vacuum. These values are slightly smaller than that of TCNQ, indicating some degree of bond-length equalization. Calculations of these values in MeCN gave greatly reduced δr numbers of 0.053 (**4**) and 0.033 (**5**) Å, which are comparable or even smaller than the corresponding values of their formally aromatic aniline donors (0.043 and 0.049 Å, respectively)! The smaller δr for the quinoid ring and larger δr for the aniline donor of **5**, compared to **4**, are in accordance with the greater degree of ground-state charge transfer in **5**. Additionally, a large dihedral angle of 24° between the two hexagonal spacers of **5** was found in

MeCN (13° in vacuum); this number is close to the twisting of aromatic biphenyl derivatives.

The interplay of the quinoid radiaannulene ring and its push–pull substituents could be seen by comparing the X-ray crystal structures of **6b** with those of symmetrically substituted **22**,[25a] **23**,[25a] and **24**,[25b] and other related molecules (Table 4; structures **22**–**24** are shown here). The average length of the endocyclic CC single bonds in **6b** is slightly shorter than of those of the symmetric compounds **22**–**24**, and also shorter than the corresponding CC single bonds of push–pull compound **20a**; the lengths of the endocyclic CC triple bonds and the exocyclic CC double bonds in **6b** are uniformly longer than those of **22**–**24** and the corresponding bonds of **20a** as well. The comparison between the endocyclic C_{sp^2}=C_{sp^2} bonds cannot be easily made, since those bonds of **22**–**24** are part of the highly aromatic benzene rings; however, the endocyclic C_{sp^2}=C_{sp^2} bond of **6b** is apparently shorter than the corresponding bonds in **20a**.

Table 4. Selected bond lengths of ethynediyl-expanded molecules **6b**, **19a**, **20a**, and **22**–**24**; standard uncertainties are given in parenthesis.

	Average bond length [Å]			
	C_{sp}–C_{sp^2}	C_{sp^2}=C_{sp^2}(*exo*)	C_{sp^2}=C_{sp^2}(*endo*)	C_{sp}≡C_{sp}
6b	1.422 (6)	1.384 (6)	1.349 (6)[a]	1.203 (6)
22	1.432 (2)	1.367 (2)	1.411 (2)[b]	1.199 (2)
23	1.430 (3)	1.369 (3)	1.409 (3)[b]	1.199 (3)
24	1.432 (7)	1.376 (7)	1.409 (8)[b]	1.195 (7)
20a	1.455 (13)	1.354 (12)	1.362 (13)[a]	1.127 (12)
19a	1.424 (3)	1.391 (3)	1.357 (3)[a]	1.208 (3)

[a] C_{sp^2}=C_{sp^2} bond in the cyclopentenyl rings, a formal double bond. [b] Benzo-annulated C_{sp^2}–C_{sp^2} bond, a formal 1.5 bond.

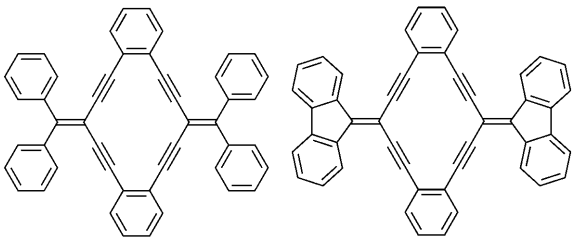

22 **23**

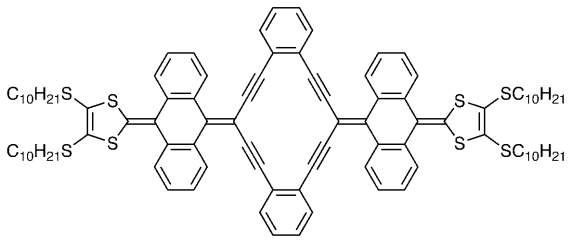

24

The shortening of the formal CC single bonds and the elongation of the formal CC double and triple bonds in macrocycle **6b** is the first experimental, structural implication of aromatization in a quinoid radiaannulene system. It should be emphasized here that all the previously proposed geometric indices of aromaticity (Julg's value, for instance)[26] are implicitly based on the assumption of bond-length equalization as a measure of aromaticity; as a result, they are applicable to systems bearing simply alternating single and double bonds. Since the concept of "bond-length equalization" is inappropriate for systems such as dehydroannulenes or radiaannulenes, which contain CC triple bonds as structural units; more structures of aromatic dehydroannulenes and radiaanulenes should be analyzed to give another way to estimate their degree of electron delocalization.

For donor substituted radiaannulene **19a**, as expected, the buta-1,3-diyne-diyl segment deviates from linearity; an average bond-angle of 167.1 (2)° was observed at each of the four C_{sp} centers. As a result, the C_{sp}-rich strained ring system exhibits electron-accepting power and polarizes its DMA donors, which have similar BLA number compared to those of **6b**. Though weakly strained, the molecule is stable not only under ambient condition, but also towards Bergman cyclization. Bergman cyclization is known to occur under physiological conditions when the terminal acetylenic atoms of endiynes are separated by 3.15–3.31 Å;[27] numbers larger than this range suggest that heating is necessary for cyclization. In the case of bis-endiyne moieties in **19a**, distances of C2–C10 (3.826 Å) and C11–C19 (3.959 Å) are longer than the optimal number. Indeed, only traces of molecules corresponding to [**19a**+H_2] or [**19a**+2H_2] were detected by mass spectroscopy after heating **19a** in cyclohexa-1,4-diene at reflux for weeks.[28]

Evidence of electron delocalization based on nucleus-independent chemical shifts (NICS) and aromatic stabilization energies (ASE): In addition to experimental characterizations presented in previous sections, symmetric and asymmetric quinoids, diphenoquinoids, and expanded quinoids, which include compounds **4**, **5**, and truncated **6**, respectively, were subjected to NICS and ASE calculations to examine the proposed concept of proaromatization in these systems. Nucleus-independent chemical shifts (NICS) were introduced by Schleyer and co-workers as a measure of electron delocalization and induced ring current.[29] This index is defined as the negative value of the calculated magnetic shielding of the dummy atoms assigned at the specific positions of interest; frequently, positions at the ring center (NICS(0)) or at 1 Å above the center relative to the ring plane (NICS(1)) are chosen. A negative NICS value is indicative of the presence of diatropic ring current; as references, the NICS(0) of highly aromatic benzene is −8.03 ppm, about +20 ppm for antiaromatic D_{2h}-cyclobutadiene, and +1.7 ppm for non-aromatic *para*-quinodimethane. The NICS calculations have been done for many annulenic compounds, but few analogous calculations were conducted for dehydroannulenes and radiaannulenes that bear acetylenic units.

Table 5. Isotropic NICS(0) values calculated in vacuum at GIAO-B3LYP/6-311+G(d,p)//B3LYP/6-31G(d) level of theory for quinoid-type molecules with various ring sizes and containing electronically symmetric or asymmetric substituents. Values calculated in MeCN are indicated.

Entry	Class	R^1	R^2	NICS(0) [ppm]
1		CN	CN	+0.66
2	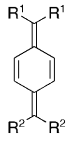	NH_2	NH_2	+3.04
3		CN	NH_2	−1.79 (vacuum) −4.90 (MeCN)
4		CN	NH_3^+	−0.86[a]
5		CN	$PhNMe_2$	−0.83 (vacuum) −3.11 (MeCN)
6		CN	$PhNMe_2H^+$	+1.07[a]
7	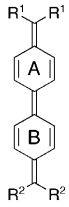	CN	NH_2	A: −1.58 B: −1.13
8		CN	$PhNMe_2$	A: −1.80 B: −1.16 (vacuum) A: −4.67 B: −4.52 (MeCN)
9		CN	$PhNMe_2H^+$	A: −0.19 B: −0.07[a]
10	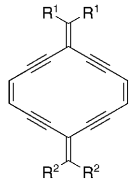	CN	CN	+0.56
11		NH_2	NH_2	+2.88
12		CN	NH_2	−3.76
13		CN	NH_3^+	−1.13[a]
14		$PhNO_2$	$PhNH_2$	−0.97
15		CN	$PhNH_2$	−2.64

[a] Geometries of the dicationic molecules were optimized at B3LYP/6-311+G(d,p).

Isotropic NICS(0) indices of quinoid-type molecules with various ring sizes and substituents were calculated; the values are shown in Table 5. NICS(1) was not used here, since we found that the number is highly contaminated by the contribution from the magnetic anisotropy of CN groups. Calculations were performed with Gaussian 09 at the GIAO-B3LYP/6-311+G(d,p)//B3LYP/6-31G(d) level of theory; symmetry constraints were not imposed. Positive NICS(0) values were found for the electronically symmetric compounds (entries 1, 2, 10, and 11). Moving to the asymmetric molecules (entries 3, 5, 7, 8, 12, 14, and 15), negative NICS(0) values ranging from −0.8 to −3.8 ppm were obtained. Calculated in high-dielectric acetonitrile, NICS(0) indices for the asymmetric molecules were even more negative (entries 3, 5, and 8), implying the greater degree of aromaticity in the more charge-separated quinoid molecules. This finding is parallel to the solvent effect on the BLA (δr) values, and highlights the interplay between ICT interaction and electron delocalization.

In silico protonation was attempted to diminish the electron-donating power of the amino groups. As depicted by entries 4, 6, 9, and 13 in Table 5, the resulting NICS(0) values became less negative compared to the corresponding neutral species; in particular, protonation of **4** (entry 6) even reverses its sign of NICS(0) to positive. These variations of NICS(0) again emphasize the necessity of having both the electron-donating and -accepting substituents to create a diatropic magnetic environment in the quinoid-type molecules. The seemingly incomplete quenching of the electron-donating power was not too surprising: based on spectroscopic evidence, Bunz and co-workers recently found that protonated *N*,*N*-dibutylanilino groups behave similarly to the weakly electron-donating phenol.[30]

Too much interpretation about the degree of aromatization should not be made based on the absolute NICS values. The ring-size and the anisotropic effects from the C≡N, C=C, and C≡C functionalities all contribute to the overall magnetic properties of the system. However, observations of 1) the homogeneous sign reversal from the positive values to the negative ones, which accompanies electronically asymmetric substitution, and 2) the much more negative NICS values for the asymmetric molecules in MeCN both clearly support the arguments of proaromaticity.

Besides the magnetic criteria of aromaticity, it has long been recognized that the resonance stabilization energy present in the π systems is an essential indication for the existence of aromaticity. Though compared to NICS, an appreciably good quality of aromatic stabilization energy (ASE) is much more difficult to reach computationally; the extent of resonance stabilization of proaromaticity was evaluated here within the scheme of hyperhomodesmotic reactions.

A hyperhomodesmotic reaction was originally designed to predict/examine the thermochemistry of hydrocarbons. The reaction is balanced under two requirements to minimize the systematic errors from the methods of calculation/experiment. It has 1) the same number of each bond type (C–C, C–CH, $C–CH_2$, $H_2C–CH_2$, C=C, HC=CH, etc.), and 2) the same number of each carbon atom types (C_{sp^3}, $C_{sp^3}(H)$, $C_{sp^3}(H_2)$, $C_{sp^3}(H_3)$, C_{sp^2}, $C_{sp^2}(H)$, $C_{sp^2}(H_2)$, etc.) in products as in reactants.[31] The concept of constructing an error-canceling reaction to predict molecular thermochemistry has also been applied to molecules containing heteroatoms.

The aromatic stabilization energies were inferred from the computed reaction energies of the hyperhomodesmotic reactions shown in Table 6; positive numbers indicate stabilization favoring the reactant side. Even though unlimited

Table 6. Hyperhomodesmotic reaction energies (zero-point energy (ZPE) corrected) as the estimates for the aromatic stabilization energies (ASEs) of quinoid molecules. Methods are indicated, and DFT calculation was performed at B3LYP/6-31G(d).

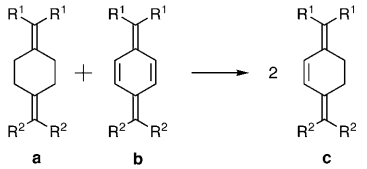

Entry	R^1	R^2	$\Delta[E(DFT)+ZPE]$ [kcal mol^{-1}]	ΔE_0(G3MP2) [kcal mol^{-1}]
1	CN	$PhNMe_2$	1.29 (vacuum) 3.71 (MeCN)	–
2	H	H	–	2.87
3	CN	CN	–	2.55
4	NH_2	NH_2	–	0.21
5	CN	NH_2	–	0.97 (vacuum) 6.67 (MeCN)

number of hyperhomodesmotic reactions could in principle be written, the chosen reaction is expected to extract only the electronic effect of the quinoid π spacer with push–pull substituents by comparing itself with the non-quinoid analogues. Here, effects from molecular sizes, the longest conjugation paths, hyperconjugation, ring-strain, allylic strain, and any other geometrical factors are preserved at both ends of the equations.

For the large systems (Table 6, entry 1), the zero-point corrected reaction energies in vacuum and in acetonitrile were calculated for the optimized structures at B3LYP/6-31G(d) level of theory. For the small ones (entries 2–5), the highly accurate, yet economic compound method of G3MP2[32] was used to reproduce effectively QCISD(T)/G3 large energies. For all calculations, vibration analysis was done to establish that a stationary point on the potential energy surface was located.

As shown in Table 6, there is a small amount of stabilization for the prototypical molecule **4** (1.29 kcal mol^{-1}); as expected, the number becomes larger in acetonitrile (3.71 kcal mol^{-1}). By comparing the valence structures of the molecules under study, the stabilization here suggests an observable stabilization of the push–pull quinoid, even though this number is much smaller in magnitude than the generally accepted approximate 36 kcal mol^{-1} resonance energy for benzene. Since such small numbers are on the order of the mean absolute deviation (MAD) of B3LYP/6-31G(d) (7.9 kcal mol^{-1} assessed on G2 molecule set),[33] model chemistry of G3MP2 at higher level of theory was sought. Due to the rather expensive computational resources needed for G3MP2, small molecules with simply C≡N as acceptors and NH_2 as donors bridged by hexagonal spacers were considered, and the electronically neutral (Table 6, entry 2), symmetric (entries 3–4), and asymmetric (entry 5) cases were treated. Surprisingly, in the gas-phase calculation, small values of stabilization resulted (0.21–2.87 kcal mol^{-1}; for G3MP2, MAD ≈1.3 kcal mol^{-1}),[32a] irrespective to the pattern of substituents, in contrast to our inferences based on spectroscopic data and findings from NICS calculations. Nonetheless, upon inclusion of solvent effects, a much greater value for the stabilization in the D-Q-A case was found, 6.67 kcal mol^{-1} (reaction 5), with an approximate sixfold increase. The ASEs we obtained here reflect the subtlety of "proaromatic stabilization" for the quinoid molecules, while the effects of electronically asymmetric substitution are more perceptible in terms of the strength of ring currents (NICS indices). Only when applying large basis sets (including diffuse functions) and consideration of solvent effect were noticeable energetic effects of proaromatization found. The difficulty in elucidating aromaticity by energetic means has been pointed out by Prof. Schleyer: "The difficulty in writing about aromaticity is that it is encrusted by two centuries of tradition … Energetic properties are most important, but you need to keep in mind that aromaticity is only 5% of the total energy. But if you want to get as close to the phenomenon as possible, then one has to go to the property most closely related, which is magnetic properties."[34]

Conclusion

Combining experimental and theoretical approaches, the push–pull quinoid D-Q-A systems were found to possess highly charge-separated ground-state characters, small HOMO–LUMO gaps, and noticeable degrees of aromaticity. Evidence of proaromaticity has been presented herein based on structural, spectroscopic, electrochemical, and computed data. The effect of proaromaticity is subtle, yet readily noticeable, even in the expanded quinoid macrocycle; in fact, compound **6** represents the first member of the radiaannulenes for which a certain degree of aromaticity is demonstrated. Although evidence from IR, NMR, and absorption spectra, electrochemistry, X-ray structures, and NICS calculations provide support and insights for proaromaticity, as shown above, a more well-designed theoretical treatment is clearly needed to describe the energetics of these systems. Experiments to test the first- and second-order molecular hyperpolarizabilities of our systems are being sought. This work provides the impetus for further application of quinoid π spacers in molecular wires in the context of molecular electronics.

Experimental Section

Materials and general methods: Reagents were purchased at reagent grade from Acros, Sigma–Aldrich, and Fluka and used as received. THF was freshly distilled from Na/benzophenone and CH_2Cl_2 from CaH_2 under N_2 atmosphere. Flash column chromatography (FC) was carried out with SiO_2 60 (particle size 0.040–0.063 mm, 230–400 mesh; Fluka) and technical solvents. Thin-layer chromatography (TLC) was conducted on aluminum sheets or glass plate coated with SiO_2 60 F_{254} obtained from Merck; visualization with a UV lamp (254 nm). Melting points (m.p.) were measured on a Büchi B-540 melting-point apparatus in open capillaries and were uncorrected; decomp indicates decomposition. ^{1}H NMR and ^{13}C NMR spectra were measured on a Varian Gemini 300, Varian Mercury 300, Bruker DRX 400, Bruker AV 400, or Bruker Avance III 600 instrument at 20 °C. Chemical shifts were reported in ppm relative to the signal of tetramethylsilane. Residual solvent signals in the ^{1}H and ^{13}C NMR spectra were used as an internal reference. Coupling constants (J) were given in Hz. The apparent resonance multiplicity was described as s (singlet), d (doublet), t (triplet), tt (triplet of triplet), and m (multiplet). Infrared spectra (IR) were recorded on a Perkin–Elmer Spectrum One FTIR Spectrometer. UV/Vis spectra were recorded on a Varian Cary-500 spectrophotometer in a quartz cuvette (1 cm). The absorption wavelengths are reported in nm with the molar extinction coefficient ε ($M^{-1}cm^{-1}$) in parenthesis; shoulders are indicated as sh. High-resolution HR-EI-MS spectra were measured on a Hitachi–Perkin–Elmer VG-Tribrid spectrometer; HR-MALDI-MS spectra were measured on a Bruker Daltonics UltraFlex II instrument with 3-hydroxypicolinic acid (3-HPA) as matrix. The signal of the molecular ion (M^+) is reported in m/z units.

X-ray analysis: X-ray data collection was carried out on a Bruker KappaCCD diffractometer equipped with a graphite monochromator ($Mo_{K\alpha}$ radiation, $\lambda = 0.71073$ Å) and an Oxford Cryostream low-temperature device. Cell dimensions were obtained by least-squares refinement of all measured reflections (HKL, Scalepack[35a]), $\theta_{max} = 27.5°$. All structures were solved by direct methods (SIR97[35b]). All non-hydrogen atoms were refined anisotropically, H-atoms isotropically by full matrix least-squares with SHELXL-97[35c] using experimental weights ($1/[\sigma^2(I_o)+(I_o+I_c)^2/900]$).

X-ray crystal structure of compound ***6b***: Single crystals were obtained by slow evaporation of a solution of **6b** in $CDCl_3$ at room temperature:

$(C_{62}H_{64}N_4O_4)_2{\cdot}(CDCl_3)_5$, $M_r = 2460.31$, crystal dimensions $0.3 \times 0.075 \times 0.015$ mm, triclinic space group $P\bar{1}$, $Z = 1$, $a = 10.2879$ (3), $b = 14.0169$ (3), $c = 22.1651$ (8) Å, $\alpha = 81.7157$ (8), $\beta = 78.2439$ (13), $\gamma = 81.6699$ (14)°, $V = 3074.5$ (2) Å^3 at 173 K. Number of measured and unique reflections 17945 and 10408, respectively ($R_{int} = 0.068$). Final $R(F) = 0.0995$, $wR(F^2) = 0.2540$ for 816 parameters and 7793 reflections with $I > 2\sigma(I)$ (corresponding R values based on all 10408 reflections 0.1290 and 0.2682).

X-ray crystal structure of compound ***19a***: Single crystals were obtained by slow diffusion of pentane into a solution of **19a** in THF at room temperature: $C_{36}H_{32}N_2{\cdot}C_4H_8O$, $M_r = 564.773$, crystal dimensions $0.18 \times 0.15 \times 0.03$ mm, orthorhombic space group *Pbcn*, $Z = 8$, $a = 32.7508$ (6), $b = 12.5342$ (2), $c = 15.0546$ (3) Å, $V = 6180.0$ (2) Å^3 at 123 K. Number of measured and unique reflections 13032 and 7009, respectively ($R_{int} = 0.062$). Final $R(F) = 0.0628$, $wR(F^2) = 0.1631$ for 516 parameters and 4714 reflections with $I > 2\sigma(I)$ (corresponding R values based on all 7009 reflections 0.1022 and 0.1922).

X-ray crystal structure of compound ***20a***: Single crystals were obtained by slow evaporation of a solution of **20a** in a mixture of Et_2O, CH_2Cl_2, and hexane at room temperature; crystals probably lost solvent molecules before measurement; cavities in the crystals are big enough for Et_2O, CH_2Cl_2 with some electron density: $C_{64}H_{48}Br_2N_6O_8$, $M_r = 1188.930$, crystal dimensions $0.3 \times 0.06 \times 0.045$ mm, monoclinic space group $P2_1/c$, $Z = 4$, $a = 14.3098$ (5), $b = 19.1052$ (8), $c = 22.9260$ (10) Å, $\beta = 94.449$ (2)°, $V = 6248.9$ (4) Å^3 at 223 K. Number of measured and unique reflections 26658 and 8023, respectively ($R_{int} = 0.107$). Final $R(F) = 0.1028$, $wR(F^2) = 0.2556$ for 721 parameters and 4239 reflections with $I > 2\sigma(I)$ (corresponding R values based on all 8023 reflections 0.1722 and 0.2942).

CCDC-773117 (**6b**), -773119 (**19a**), and -773118 (**20a**) contain the supplementary crystallographic data for this paper. These data can be obtained free of charge from The Cambridge Crystallographic Data Centre via www.ccdc.cam.ac.uk/data_request/cif.

Electrochemistry: Electrochemical measurements were carried out in CH_2Cl_2 containing 0.1 M nBu_4NPF_6 in a classical three-electrode cell by cyclic voltammetry (CV) and rotating-disk voltammetry (RDV). The working electrode was a glassy carbon disk (3 mm in diameter), the auxiliary electrode a Pt wire, and the pseudo reference electrode a Pt wire. The cell was connected to an Autolab PGSTAT30 potentiostat (Eco Chemie, Holland) driven by a GPSE software running on a personal computer. All potentials are referenced to the ferricinium/ferrocene (Fc^+/Fc) couple used as internal standard and are uncorrected from ohmic drop.

2-(4′-Bromobiphenyl-4-yl)malononitrile (12): NaH (95%, 0.189 g, 7.5 mmol) was added in small portions to an ice-water cooled solution of malonitrile (0.363 g, 5.5 mmol) in anhydrous THF (30 mL); the suspension was then stirred under N_2 atomosphere at room temperature. After 30 min, 4,4′-dibromobiphenyl (1.56 g, 5 mmol) and $[Pd(PPh_3)_2Cl_2]$ (0.14 g, 0.2 mmol) were added and the resulting mixture was heated for 42 h at reflux. The mixture was acidified with 1 N HCl at 0 °C and extracted with CH_2Cl_2. The organic layer was dried over $MgSO_4$, the solvent removed under reduced pressure, and the residue purified by FC (SiO_2, CH_2Cl_2/hexane 1:1) to give the product as a white solid (0.83 g, 54%). M.p. 128–130 °C; ^{1}H NMR ($CDCl_3$, 300 MHz): $\delta = 5.11$ (s, 1H), 7.45 (d, $J = 8.4$ Hz, 2H), 7.58 (d, $J = 8.4$ Hz, 2H), 7.61 (d, $J = 8.4$ Hz, 2H), 7.68 ppm (d, $J = 8.4$ Hz, 2H); ^{13}C NMR ($CDCl_3$, 75 MHz): $\delta = 27.92$, 111.52, 122.59, 125.21, 127.69, 128.36, 128.63, 132.07, 138.10, 142.18 ppm; IR (neat): $\tilde{\nu} = 2922$, 2899, 2852, 2255, 1480, 1074, 1002, 821, 791 cm^{-1}; HR-EI-MS: *m/z* (%): 297.9923 (85) $[M]^+$, 295.9944 (85) $[M]^+$ (*m/z* calcd for $C_{15}H_9{}^{79}BrN_2{}^+$: 295.9944), 217.0756 (100), 190.0645 (48), 152.0616 (29).

7,7-Bis[4-(dimethylamino)phenyl]-7′,7′-dicyanodiphenoquinodimethane (5): A mixture of **12** (0.298 g, 1 mmol) in anhydrous THF (20 mL) at −78 °C under N_2 was treated with *n*BuLi (1.38 mL, 2.2 mmol, 1.6 M solution in hexane) and the resulting solution was stirred at −78 °C for 5 h to ensure the complete generation of the dianionic species. Michler's ketone (0.241 g, 0.90 mmol) was then added and the resulting mixture stirred overnight at room temperature. The crude mixture was filtered through a plug of SiO_2 (MeCN) and concentrated. Subsequent FC (SiO_2; CH_2Cl_2/MeCN 3:2) afforded **5** (216 mg, 51%) as a purple metallic solid (green in CH_2Cl_2). M.p. > 250 °C (decomp); ^{1}H NMR ($CDCl_3$, 300 MHz): $\delta = 3.31$ (s, 12H), 6.78 (d, $J = 9$ Hz, 4H), 6.87 (d, $J = 8.4$ Hz, 2H), 7.14 (d, $J = 8.4$ Hz, 2H), 7.23 (d, $J = 8.4$ Hz, 2H), 7.27 (d, $J = 9$ Hz, 4H), 7.45 ppm (d, $J = 8.4$ Hz, 2H); ^{13}C NMR ($CDCl_3$, 75 MHz): $\delta = 40.86$, 112.98, 119.65, 124.43, 125.57, 125.94, 126.51, 126.95, 135.36, 136.47, 140.26, 144.73, 146.85, 156.10, 176.72 ppm (1 signal was missing); IR (neat): $\tilde{\nu} = 2165$, 2123, 1614, 1520, 1481, 1359, 1287, 1169 cm^{-1}; UV/Vis (CH_2Cl_2): λ_{max} (ε) = 611 (105 000), 845 nm (30 500); HR-MALDI-MS: *m/z* (%): 470.2422 (31), 469.2394 (100) $[M+H]^+$ (*m/z* calcd for $C_{32}H_{29}N_4{}^+$: 469.2397).

1,1′-(2,2-Dibromoethene-1,1-diyl)bis(4-nitrobenzene) (13): Bis(4-nitrophenyl)methanone (300 mg, 1.1 mmol) was added to the solution of CBr_4 (731 mg, 2.20 mmol) and PPh_3 (1156 mg, 4.40 mmol) in anhydrous CH_2Cl_2 (50 mL) in one portion. The mixture was heated at reflux for 4 h under Ar. The crude mixture was filtered through a plug of SiO_2 (CH_2Cl_2) and concentrated. Subsequent FC (SiO_2; CH_2Cl_2/hexane 15:1) afforded **13** as a white solid (340 mg, 72%). M.p. 195–197 °C; ^{1}H NMR ($CDCl_3$, 400 MHz): $\delta = 7.50$ (d, $J = 8.5$ Hz, 4H), 8.23 ppm (d, $J = 8.5$ Hz, 4H); ^{13}C NMR ($CDCl_3$, 100 MHz): $\delta = 94.79$, 123.97, 129.88, 143.83, 146.25, 147.50; IR (neat): $\tilde{\nu} = 2924$, 1603, 1523, 1344, 1106, 704 cm^{-1}; HR-EI-MS: *m/z* (%): 429.8806 (51) $[M]^+$, 427.8833 (100) $[M]^+$, 425.8844 (49) $[M]^+$ (*m/z* calcd for $C_{14}H_8{}^{79}Br_2N_2O_4{}^+$: 425.8851), 268.0468 (36), 176.0618 (61).

***N,N*-Dibutyl-4-(4,4,5,5-tetramethyl-1,3,2-dioxaborolan-2-yl)aniline**: A mixture of 4-bromo-*N,N*-dibutylaniline (2.416 g, 8.5 mmol) in anhydrous THF (120 mL) was slowly treated with *n*BuLi (6.4 mL, 10.2 mmol, 1.6 M solution in hexane) at −78 °C under Ar, and the resulting solution was stirred at −78 °C for 1.5 h. Triisopropyl borate (5.9 mL, 25.5 mmol) was then added in one portion to the above solution, and the temperature was slowly increased to room temperature. The mixture was stirred at this temperature overnight, and subsequently sat. $NH_4Cl_{(aq)}$ (80 mL) was added. After 2 h of stirring, the mixture was extracted with CH_2Cl_2. The organic phase was collected, dried over Na_2SO_4, and concentrated, and the residue was re-dissolved in a solution of NH_4Cl (0.7 g, 13 mmol) and pinacol (1.310 g, 11.05 mmol) in anhydrous toluene (80 mL). The mixture was heated at reflux for 9 h. After cooling, the mixture was extracted with H_2O and CH_2Cl_2. The organic phases were collected, dried over Na_2SO_4, and the residue was purified by FC (SiO_2; CH_2Cl_2/hexane 1:2→1:1) to give the title product as white solid (1.872 g, 66%). M.p. ≈30 °C; ^{1}H NMR ($CDCl_3$, 300 MHz): $\delta = 0.94$ (t, $J = 7.3$ Hz, 6H), 1.26–1.41 (m, 4H), 1.31 (s, 12H), 1.51–1.61 (m, 4H), 3.28 (t, $J = 7.5$ Hz, 4H), 6.60 (d, $J = 8.9$ Hz, 2H), 7.64 ppm (d, $J = 8.9$ Hz, 2H); ^{13}C NMR ($CDCl_3$, 75 MHz): $\delta = 14.24$, 20.52, 25.01, 29.54, 50.60, 53.50, 82.98, 110.43, 136.03, 149.98 ppm; IR (neat): $\tilde{\nu} = 2959$, 2932, 2870, 1601, 1399, 1351, 1142, 1094, 861, 814, 655 cm^{-1}; HR-MALDI-MS: *m/z* (%): 408.3509 (35), 322.2757 (69) $[M+H]^+$ (*m/z* calcd for $C_{20}H_{35}BNO_2{}^+$: 332.2755), 235.0709 (100).

4,4′-{4-(Triisopropylsilyl)-2-[(triisopropylsilyl)ethynyl]but-1-en-3-yne-1,1-diyl}bis(*N,N*-dimethylaniline) (15a): A solution of **14** (331 mg, 0.606 mmol), 4-(*N,N*-dimethylamino)benzeneboronic acid (300 mg, 1.818 mmol), $[Pd(PPh_3)_2Cl_2]$ (43 mg, 0.06 mmol), and Na_2CO_3 (193 mg, 1.82 mmol) in THF/H_2O (10 mL, 4:1) was stirred at 70 °C under Ar overnight. The mixture was extracted with H_2O and CH_2Cl_2, and the organic layers were collected and the solvents removed under reduced pressure. The residue was purified by collecting the yellow portions from FC (SiO_2, CH_2Cl_2/hexane 1:5→1:3) (360 mg, 95%). M.p. 112–114 °C; ^{1}H NMR ($CDCl_3$, 400 MHz): $\delta = 1.10$ (s, 42H), 3.30 (s, 12H), 6.65 (d, $J = 8.9$ Hz, 4H), 7.48 ppm (d, $J = 8.9$ Hz, 4H); ^{13}C NMR ($CDCl_3$, 100 MHz): $\delta = 11.45$, 18.68, 40.35, 92.23, 97.05, 107.38, 111.01, 128.47, 131.98, 150.36, 156.94 ppm; IR (neat): $\tilde{\nu} = 2939$, 2886, 2860, 2141, 2119, 1604, 1461, 1162, 816, 672 cm^{-1}; HR-MALDI-MS: *m/z* (%): 628.4545 (46), 627.4524 (100) $[M+H]^+$ (*m/z* calcd for $C_{40}H_{63}N_2Si_2{}^+$: 627.4524), 626.4472 (74) $[M]^+$.

4,4′-{4-(Triisopropylsilyl)-2-[(triisopropylsilyl)ethynyl]but-1-en-3-yne-1,1-diyl}bis(*N,N*-dibutylaniline) (15b): A solution of **14** (1048 mg, 1.917 mmol), *N,N*-dibutyl-4-(4,4,5,5-tetramethyl-1,3,2-dioxaborolan-2-yl)aniline (1905 mg, 5.752 mmol), and Na_2CO_3 (620 mg, 5.752 mmol) in THF/H_2O (30 mL, 5:1) was purged with Ar for 25 min. $[Pd(PPh_3)_4]$ (200 mg, 0.173 mmol) was added to the above mixture, and the solution was purged with Ar for another 15 min. The mixture was stirred at 70 °C

overnight and then extracted with H_2O and CH_2Cl_2. After removal of the solvents, preliminary ^1H NMR analysis indicated a mixture of starting dibromo compound and partially reacted monoanilino-substituted compound present in the residue. Thus, the residue (ca. 500 mg) and **14** (484 mg, 0.886 mmol) were again reacted with *N,N*-dibutyl-4-(4,4,5,5-tetramethyl-1,3,2-dioxaborolan-2-yl)aniline (1410 mg, 4.26 mmol), Na_2CO_3 (450 mg, 4.26 mmol), and $[Pd(PPh_3)_4]$ (200 mg, 0.173 mmol) according to the procedure described above. The mixture was heated at 80 °C for 3 d, and the product was purified according to the method described for **15a** (1827 mg, 82 %). M.p. 96–98 °C; ^1H NMR ($CDCl_3$, 400 MHz): $\delta = 0.95$ (t, $J = 7.3$ Hz, 12H), 1.03 (s, 42H) 1.27–1.41 (m, 8H), 1.50–1.62 (m, 8H), 3.26 (t, $J = 7.5$ Hz, 8H), 6.49 (d, $J = 9.0$ Hz, 4H), 7.39 ppm (d, $J = 9.0$ Hz, 4H); ^{13}C NMR ($CDCl_3$, 100 MHz): $\delta = 11.48$, 13.97, 18.67, 20.33, 29.47, 50.74, 91.73, 95.89, 107.81, 110.04, 127.11, 132.24, 148.06, 157.49 ppm; IR (neat): $\tilde{\nu} = 2938$, 2861, 2131, 1600, 1519, 1189, 813, 674 cm^{-1}; HR-MALDI-MS: *m/z* (%): 796.6429 (55), 795.6398 (100) $[M+H]^+$ (*m/z* calcd for $C_{52}H_{87}N_2Si_2^+$: 795.6402), 794.6334 (51) $[M]^+$.

2,2′-(3-{Bis[4-(dimethylamino)phenyl]methylene}penta-1,4-diyne-1,5-diyl)biscyclopent-1-ene-1-carbaldehyde (17a): A solution of TBAF·3 H_2O (252 mg, 0.80 mmol) and the TIPS-protected ethynyl compound **15a** (100 mg, 0.16 mmol) in THF (15 mL) was stirred at room temperature for 40 min. The mixture was extracted with H_2O and CH_2Cl_2, and the terminal acetylene compound was obtained from the organic layer. The diethynyl intermediate obtained from the above operation was mixed with **16** (70 mg, 0.40 mmol), $[Pd(PPh_3)_4]$ (20 mg, 0.016 mmol), CuI (5.7 mg, 0.030 mmol), THF (1.5 mL), and Et_3N (15 mL). The solution was stirred at room temperature overnight, while the color of the mixture quickly turned deep red. The mixture was passed through a pad of SiO_2 (MeCN). After concentration under reduced pressure, the residue was purified by FC (SiO_2, $CH_2Cl_2 \rightarrow CH_2Cl_2$/MeCN 2:3) to afford **17a** as red solid (80 mg, 99 %). M.p. 178–180 °C; ^1H NMR ($CDCl_3$, 300 MHz): $\delta = 1.87$–2.02 (m, 4H), 2.58 (t, $J = 8.0$ Hz, 4H), 2.70 (t, $J = 6.0$ Hz, 4H), 3.02 (s, 12H), 6.63 (d, $J = 9.0$ Hz, 4H), 7.39 (d, $J = 9.0$ Hz, 4H), 9.61 ppm (s, 2H); ^{13}C NMR ($CDCl_3$, 100 MHz): $\delta = 22.27$, 29.48, 38.52, 40.22, 84.91, 93.40, 102.49, 110.70, 127.33, 132.60, 143.52, 147.02, 151.39, 162.80, 189.30 ppm; IR (neat): $\tilde{\nu} = 2900$, 2848, 2807, 2176, 2154, 1655, 1596, 1360, 822, 813 cm^{-1}; HR-MALDI-MS: *m/z* (%): 504.2726 (41), 503.2684 (100) $[M+H]^+$ (*m/z* calcd for $C_{34}H_{35}N_2O_2^+$: 503.2693), 502.2599 (23) $[M]^+$.

2,2′-(3-{Bis[4-(dibutylamino)phenyl]methylene}penta-1,4-diyne-1,5-diyl)-biscyclopent-1-ene-1-carbaldehyde (17b): The synthesis is similar to that described for **17a**. The TIPS groups of **15b** (1.77 g, 2.23 mmol) were removed by reacting it with TBAF·3 H_2O (3.51 g, 11.13 mmol) in THF (80 mL) for 1.5 h. The diethynyl intermediate obtained from extraction was mixed with **16** (976 mg, 5.58 mmol), $[Pd(PPh_3)_2Cl_2]$ (160 mg, 0.23 mmol), CuI (87 mg, 0.46 mmol), THF (3 mL), and Et_3N (30 mL). After purification by FC (SiO_2, $CH_2Cl_2 \rightarrow CH_2Cl_2$/MeCN 2:3), the butyl product **17b** was obtained as red solid (1 g, 67 %). M.p. 125–127 °C; ^1H NMR ($CDCl_3$, 400 MHz): $\delta = 0.96$ (t, $J = 7.3$ Hz, 12H), 1.30–1.44 (m, 8H), 1.54–1.66 (m, 8H), 1.93 (tt, $J = 7.7$, 7.7 Hz, 4H), 2.58 (t, $J = 7.5$ Hz, 4H), 2.69 (t, $J = 7.6$ Hz, 4H), 3.31 (t, $J = 8.0$ Hz, 8H), 6.56 (d, $J = 9.0$ Hz, 4H), 7.38 (d, $J = 9.0$ Hz, 4H), 9.70 ppm (s, 2H); ^{13}C NMR ($CDCl_3$, 100 MHz): $\delta = 13.92$, 20.27, 22.22, 29.32, 29.41, 38.49, 50.72, 84.79, 91.96, 103.12, 109.93, 126.02, 132.92, 143.60, 146.50, 149.29, 163.01, 189.10 ppm; IR (neat): $\tilde{\nu} = 2954$, 2928, 2869, 2176, 2160, 1655, 1597, 1522, 1356, 1189, 815 cm^{-1}; HR-MALDI-MS: *m/z* (%): 672.4618 (54), 671.4581 (100) $[M+H]^+$ (*m/z* calcd for $C_{46}H_{59}N_2O_2^+$: 671.4571), 670.4501 $[M]^+$.

4,4′-{[14-[Bis(4-nitrophenyl)methylene]-4,5,7,8,12,13,15,16-octadehydro-2,3,9,10,11,14-hexahydrodicyclopenta[*a*,*h*]cyclotetradecen-6(1*H*)-ylidene]methylene}bis(*N*,*N*-dimethylaniline) (6a): A solution of TMSC(Li)N_2 was freshly prepared by reacting lithium diisopropylamide (150 μL, 0.27 mmol, 1.8 M in THF/heptane/ethylbenzene) with trimethylsilyldiazomethane (150 μL, 0.30 mmol, 2.0 M in Et_2O) in anhydrous THF (5 mL) at −78 °C for 30 min. A mixture of **17a** (60 mg, 0.12 mmol) in anhydrous THF (5 mL) was then introduced to the above solution. The whole mixture was stirred at −78 °C for 1 h, followed by heating at reflux for 3 h. After cooling, the mixture was extracted with water and CH_2Cl_2. The organic layers were collected and dried over Na_2SO_4, solvents were removed under reduced pressure, and the residue was purified by a short pad of SiO_2 (CH_2Cl_2/hexane 5:1) to give diethynylated **18a**. A 1:1 mixture of anhydrous Et_3N/THF (15 mL) was freshly subjected to the freeze-pump-thaw cycle 5 times before use. The inner atmosphere of the flask containing **18a**, from the previous transformation, **13** (51 mg, 0.12 mmol), CuI (3 mg, 0.014 mmol), and $[Pd(PPh_3)_4]$ (8 mg, 0.007 mmol) was changed to Ar by three evacuation-refilling cycles. The oxygen-free Et_3N/THF mixture was then introduced to the above flask, and the mixture was heated at 70 °C for 24 h under Ar. After cooling, the crude mixture was passed through a pad of SiO_2 (MeCN). After concentration under reduced pressure, the residue from the filtrate was purified by FC (SiO_2, CH_2Cl_2/hexane 1:1→CH_2Cl_2) to afford **6a** as green metallic solid (35 mg, 38 %). M.p. > 400 °C; ^1H NMR ($CDCl_3$, 600 MHz): $\delta = 1.85$–1.97 (m, 4H), 2.45 (t, $J = 6.2$ Hz, 4H), 2.52 (t, $J = 7.1$ Hz, 4H), 3.02 (s, 12H), 6.64 (br s, 4H), 7.46 (d, $J = 9.0$ Hz, 4H), 7.67 (d, $J = 9.0$ Hz, 4H), 8.20 ppm (d, $J = 9.0$ Hz, 4H); ^{13}C NMR ($CDCl_3$, 150 MHz): $\delta = 35.66$, 36.49, 40.28, 87.75, 93.36, 95.26, 100.98, 108.33, 110.52, 123.15, 127.31, 127.93, 131.21, 132.81, 134.90, 145.29, 146.11, 147.33, 158.19 ppm (3 peaks were missing); IR (neat): $\tilde{\nu} = 2920$, 2850, 2162, 1600, 1512, 1469, 1331, 1187 cm^{-1}; UV/Vis (CH_2Cl_2): λ_{max} (ε) = 586 nm (38500); HR-MALDI-MS: *m/z* (%): 762.3153 (46), 761.3111 (100) $[M+H]^+$ (*m/z* calcd for $C_{50}H_{41}N_4O_4^+$: 7601.3122), 760.3056 (91) $[M]^+$, 745.3193 (24).

4,4′-{[14-[Bis(4-nitrophenyl)methylene]-4,5,7,8,12,13,15,16-octadehydro-2,3,9,10,11,14-hexahydrodicyclopenta[*a*,*h*]cyclotetradecen-6(1*H*)-ylidene]methylene}bis(*N*,*N*-dibutylaniline) (6b): The synthesis of **18b** was performed by using the method described for **18a**. Lithium diisopropylamide (0.56 mL, 1.0 mmol, 1.8 M in THF/heptane/ethylbenzene), trimethylsilyldiazomethane (0.56 mL, 1.12 mmol, 2.0 M in Et_2O) THF (15 + 8 mL) were used to prepare **16b** (300 mg, 0.447 mmol). An oxygen-free 3:1 mixture of anhydrous Et(*i*Pr)$_2$N/THF (15 mL) was freshly prepared by freeze-pump-thaw cycles. The inner atmosphere of the flask containing **18b** (93 mg, 0.14 mmol), **13** (60 mg, 0.14 mmol), CuI (3 mg, 0.014 mmol), and $[Pd(PPh_3)_4]$ (8 mg, 0.007 mmol) was changed to Ar by three evacuation-refilling cycles. The solvent was then introduced to the above flask and the mixture heated at 90 °C for 24 h under Ar. After cooling, the crude mixture was passed through a pad of SiO_2 (MeCN). After concentration under reduced pressure, the residue was purified by FC (SiO_2, CH_2Cl_2/hexane 2:3→1:1) to afford **6b** as green metallic solid (25 mg, 19 %). The formation of **19b** and **20b** was not observed. M.p. 261–262 °C; ^1H NMR ($CDCl_3$, 300 MHz): $\delta = 0.97$ (t, $J = 7.3$ Hz, 12H), 1.30–1.43 (m, 8H), 1.53–1.66 (m, 8H), 1.84–1.98 (m, 4H), 2.43–2.56 (m, 8H), 3.32 (t, $J = 7.5$ Hz, 8H), 6.55 (d, $J = 9.0$ Hz, 4H), 7.44 (d, $J = 9.0$ Hz, 4H), 7.67 (d, $J = 9.0$ Hz, 4H), 8.18 ppm (d, $J = 9.0$ Hz, 4H); ^{13}C NMR ($CDCl_3$, 75 MHz): $\delta = 14.25$, 20.55, 23.59, 29.67, 35.77, 36.59, 50.84, 87.63, 93.46, 94.05, 95.27, 101.66, 108.25, 109.70, 122.93, 126.29, 126.59, 131.00, 132.91, 134.77, 144.64, 145.88, 146.93, 148.53, 158.59 ppm; IR (neat): $\tilde{\nu} = 2954$, 2926, 2869, 2159, 1594, 1515, 1456, 1337, 1190 cm^{-1}; HR-MALDI-MS: *m/z* (%): 930.5045, 929.5013 (100) $[M+H]^+$ (*m/z* calcd for $C_{62}H_{65}N_4O_4^+$: 929.5000), 928.4960 (75) $[M]^+$, 913.5063 (14).

4,4′-(4,5,6,7,11,12,14,15-Octadehydro-1,2,3,8,9,10-hexahydro-13*H*-dicyclopenta[*a*,*g*]cyclotridecen-13-ylidenemethylene)bis(*N*,*N*-dimethylaniline) (19a): Radiaannulene **19a** was occasionally isolated from the synthesis of **6a**; the yield is varying. M.p. > 248 °C (explosion); ^1H NMR ($CDCl_3$, 400 MHz): $\delta = 2.00$ (tt, $J = 8.0$, 8.0 Hz, 4H), 2.53 (t, $J = 8.0$ H, 8H), 3.03 (s, 12H), 6.66 (d, $J = 8.7$ Hz, 4H), 7.49 ppm (d, $J = 8.7$ Hz, 4H); ^{13}C NMR ($CDCl_3$, 100 MHz): $\delta = 23.76$, 33.68, 35.79, 40.24, 84.77, 88.49, 91.22, 94.64, 100.95, 110.50, 127.89, 128.16, 133.88, 140.17, 150.95, 161.01 ppm; IR (neat): $\tilde{\nu} = 2919$, 2846, 2182, 2160, 2124, 1596, 1521, 1467, 1357, 813 cm^{-1}; UV/Vis (CH_2Cl_2): λ_{max} (ε) = 432 (9500), 531 nm (14900); HR-MALDI-MS: *m/z* (%): 493.2605 (62), 492.2553 (100) $[M+H]^+$ (*m/z* calcd for $C_{36}H_{33}N_2^+$: 493.2638), 491.2473 (20) $[M]^+$.

4,4′-[4-{2-[3-Bromo-4,4-bis(4-nitrophenyl)but-3-en-1-yn-1-yl]cyclopent-1-en-1-yl}-2-({2-[3-bromo-4,4-bis(4-nitrophenyl)but-3-en-1-yn-1-yl]cyclopent-1-en-1-yl}ethynyl)but-1-en-3-yne-1,1-diyl]bis(*N*,*N*-dimethylaniline) (20a): Compound **20a** was occasionally isolated from the synthesis of **6a**; the yield varied and about 1 mg was collected in total. ^1H NMR ($CDCl_3$, 400 MHz): $\delta = 1.91$ (tt, $J = 7.5$, 7.5 Hz, 4H), 2.51 (t, $J = 7.5$ Hz, 4H), 2.57 (t, $J = 7.5$ Hz, 4H), 2.99 (s, 12H), 6.64 (d, $J = 9.0$ Hz, 4H), 7.39 (d, $J = 9.0$ Hz, 4H), 7.47 (d, $J = 9.0$ Hz, 8H), 8.14 (d, $J = 9.0$ Hz, 4H), 8.23 ppm

(d, $J=9.0$ Hz, 4H); ^{13}C NMR ($CDCl_3$, 100 MHz): $\delta=23.25$, 36.33, 37.44, 40.27, 87.42, 92.83, 96.17, 100.17, 103.60, 110.52, 123.44, 123.64, 125.57, 127.64, 130.68, 130.83, 132.88, 135.46, 143.55, 144.20, 147.28, 147.49, 150.95 ppm (3 peaks were missing); UV/Vis (CH_2Cl_2): λ_{max} (ε) = 504 nm (sh, 23 100); HR-MALDI-MS: *m/z* (%): 1191.2016 (40), 1190.1919 (56), 1189.1954 (67) $[M+H]^+$ (*m/z* calcd for $C_{64}H_{49}{}^{79}Br^{81}BrN_6O_8{}^+$: 1189.1958), 1188.1903 (60), 1187.1892 (48), 1186.1883 (32), 1171.1726 (20), 1111.2756 (41), 1110.2740 (72), 1109.2710 (100), 1108.2693 (74), 1107.2666 (74), 1106.2833 (42), 1093.2748 (33), 1030.3631 (45), 1029.3585 (73), 1028.3493 (85), 1027.3487 (80), 1011.3530 (43).

Acknowledgements

We are grateful for access to the Competence Center for Computational Chemistry (C4) Obelix cluster (ETH). Y.-L.W. appreciates being the recipient of a scholarship from the Schweizerischen Chemischen Industrie (SSCI). The research was funded by a grant from the ETH research council and, in part, by the ERC Advanced Grant No. 246637 ("OPTELOMAC"). We thank R. R. Tykwinski (Nürnberg–Erlangen) and K. Müllen (Mainz) for valuable discussions.

[1] a) G. Qian, Z. Zhong, M. Luo, D. Yu, Z. Zhang, Z. Y. Wang, D. Ma, *Adv. Mater.* **2009**, *21*, 111–116; b) S. T. Meek, E. E. Nesterov, T. M. Swager, *Org. Lett.* **2008**, *10*, 2991–2993; c) G. Qian, B. Dai, M. Luo, D. Yu, J. Zhan, Z. Zhang, D. Ma, Z. Y. Wang, *Chem. Mater.* **2008**, *20*, 6208–6216.

[2] a) Y. Yao, Y. Liang, V. Shrotriya, S. Xiao, L. Yu, Y. Yang, *Adv. Mater.* **2007**, *19*, 3979–3983; b) special issue on "Low-Band-Gap Polymer Materials for Organic Solar Cells": *Sol. Energy Mater. Sol. Cells* **2007**, *91*, 953–1036, edited by F. C. Krebs.

[3] a) L. Beverina, J. Fu, A. Leclercq, E. Zojer, P. Pacher, S. Barlow, E. W. V. Stryland, D. J. Hagan, J.-L. Brédas, S. R. Marder, *J. Am. Chem. Soc.* **2005**, *127*, 7282–7283; b) S. Zheng, A. Leclercq, J. Fu, L. Beverina, L. A. Padilha, E. Zojer, K. Schmidt, S. Barlow, J. Luo, S.-H. Jiang, A. K.-Y. Jen, Y. Yi, Z. Shuai, E. W. V. Stryland, D. J. Hagan, J.-L. Brédas, S. R. Marder, *Chem. Mater.* **2007**, *19*, 432–442; c) J. M. Hales, S. Zheng, S. Barlow, S. R. Marder, J. W. Perry, *J. Am. Chem. Soc.* **2006**, *128*, 11362–11363.

[4] a) D. F. Perepichka, M. R. Bryce, *Angew. Chem.* **2005**, *117*, 5504; *Angew. Chem. Int. Ed.* **2005**, *44*, 5370—5373; b) H. A. M. van Mullekom, J. A. J. M. Vekemans, E. E. Havinga, E. W. Meijer, *Mater. Sci. Eng. R* **2001**, *32*, 1–40; c) J. Roncali, *Chem. Rev.* **1997**, *97*, 173–205.

[5] a) M. Kivala, C. Boudon, J.-P. Gisselbrecht, P. Seiler, M. Gross, F. Diederich, *Chem. Commun.* **2007**, 4731–4733; b) P. Reutenauer, M. Kivala, P. D. Jarowski, C. Boudon, J.-P. Gisselbrecht, M. Gross, F. Diederich, *Chem. Commun.* **2007**, 4898–4900; c) M. Kivala, C. Boudon, J.-P. Gisselbrecht, B. Enko, P. Seiler, I. B. Müller, N. Langer, P. D. Jarowski, G. Gescheidt, F. Diederich, *Chem. Eur. J.* **2009**, *15*, 4111–4123; d) S.-i. Kato, M. Kivala, W. B. Schweizer, C. Boudon, J.-P. Gisselbrecht, F. Diederich, *Chem. Eur. J.* **2009**, *15*, 8687–8691; e) C. Koos, P. Vorreau, T. Vallaitis, P. Dumon, W. Bogaerts, R. Baets, B. Esembeson, I. Biaggio, T. Michinobu, F. Diederich, W. Freude, J. Leuthold, *Nat. Photonics* **2009**, *3*, 216–219; f) J. Leuthold, W. Freude, J.-M. Brosi, R. Baets, P. Dumon, I. Biaggio, M. L. Scimeca, F. Diederich, B. Frank, C. Koos, *Proc. IEEE* **2009**, *97*, 1304–1316; g) T. Vallaitis, S. Bogatscher, L. Alloatti, P. Dumon, R. Baets, M. L. Scimeca, I. Biaggio, F. Diederich, C. Koos, W. Freude, J. Leuthold, *Opt. Express* **2009**, *17*, 17357–17368.

[6] a) F. Wudl, N. Kobayashi, A. J. Heeger, *J. Org. Chem.* **1984**, *49*, 3382–3384; b) J.-L. Brédas, A. J. Heeger, F. Wudl, *J. Chem. Phys.* **1986**, *85*, 4673–4678; c) H. Reisch, U. Wiesler, U. Scherf, N. Tuytuylkov, *Macromolecules* **1996**, *29*, 8204–8210.

[7] a) S. R. Marder, J. W. Perry, G. Bourhill, C. B. Gorman, B. G. Tiemann, K. Mansour, *Science* **1993**, *261*, 186–189; b) S. R. Marder, L.-T. Cheng, B. G. Tiemann, A. C. Friedli, M. Blanchard-Desce, J. W. Perry, J. Skindhoj, *Science* **1994**, *263*, 511–514.

[8] R. Gompper, H.-U. Wagner, E. Kutter, *Chem. Ber.* **1968**, *101*, 4123–4143.

[9] a) R. Andreu, M. J. Blesa, L. Carrasquer, J. Garín, J. Orduna, B. Villacampa, R. Alcalá, J. Casado, M. C. R. Delgado, J. T. L. Navarrete, M. Allain, *J. Am. Chem. Soc.* **2005**, *127*, 8835–8845; b) S. Inoue, Y. Aso, T. Otsubo, *Chem. Commun.* **1997**, 1105–1106; c) S. Inoue, S. Mikami, Y. Aso, T. Otsubo, T. Wada, H. Sasabe, *Synth. Met.* **1997**, *84*, 395–396; d) T. Kawase, M. Wakabayashi, C. Takahashi, M. Oda, *Chem. Lett.* **1997**, 1055–1056; e) A. S. Batsanov, M. R. Bryce, M. A. Coffin, A. Green, R. E. Hester, J. A. K. Howard, I. K. Lednev, N. Martín, A. J. Moore, J. N. Moore, E. Ortí, L. Sánchez, M. Savirón, P. M. Viruela, R. Viruela, T.-Q. Ye, *Chem. Eur. J.* **1998**, *4*, 2580–2592.

[10] a) A. Abbotto, L. Beverina, S. Bradamante, A. Facchetti, C. Klein, G. A. Pagani, M. Redi-Abshiro, R. Wortmann, *Chem. Eur. J.* **2003**, *9*, 1991–2007; b) R. Andreu, J. Garín, J. Orduna, R. Alcalá, B. Villacampa, *Org. Lett.* **2003**, *5*, 3143–3146; c) A. J. Kay, A. D. Woolhouse, Y. Zhao, K. Clays, *J. Mater. Chem.* **2004**, *14*, 1321–1330; d) S. Alías, R. Andreu, M. J. Blesa, M. A. Cerdán, S. Franco, J. Garín, C. López, J. Orduna, J. Sanz, R. Alicante, B. Villacampa, M. Allain, *J. Org. Chem.* **2008**, *73*, 5890–5898; e) R. Andreu, M. A. Cerdán, S. Franco, J. Garín, A. B. Marco, J. Orduna, D. Palomas, B. Villacampa, R. Alicante, M. Allain, *Org. Lett.* **2008**, *10*, 4963–4966; f) J. Schmidt, R. Schmidt, F. Würthner, *J. Org. Chem.* **2008**, *73*, 6355–6362; g) R. Andreu, L. Carrasquer, S. Franco, J. Garín, J. Orduna, N. M. de Baroja, R. Alicante, B. Villacampa, M. Allain, *J. Org. Chem.* **2009**, *74*, 6647–6657; h) R. Andreu, E. Galán, J. Garín, V. Herrero, E. Lacarra, J. Orduna, R. Alicante, B. Villacampa, *J. Org. Chem.* **2010**, *75*, 1684–1692.

[11] For chemistry of radiaannulenes and expanded radialenes, see: a) M. B. Nielsen, M. Schreiber, Y. G. Baek, P. Seiler, S. Lecomte, C. Boudon, R. R. Tykwinski, J.-P. Gisselbrecht, V. Gramlich, P. J. Skinner, C. Bosshard, P. Gunter, M. Gross, F. Diederich, *Chem. Eur. J.* **2001**, *7*, 3263–3280; b) F. Mitzel, C. Boudon, J.-P. Gisselbrecht, P. Seiler, M. Gross, F. Diederich, *Chem. Commun.* **2003**, 1634–1635; c) F. Mitzel, C. Boudon, J.-P. Gisselbrecht, P. Seiler, M. Gross, F. Diederich, *Helv. Chim. Acta* **2004**, *87*, 1130–1157; d) M. Gholami, R. R. Tykwinski, *Chem. Rev.* **2006**, *106*, 4997–5027; e) F. Diederich, M. Kivala, *Adv. Mater.* **2008**, *20*, 803–812.

[12] F. Bure, W. B. Schweizer, C. Boudon, J.-P. Gisselbrecht, M. Gross, F. Diederich, *Eur. J. Org. Chem.* **2008**, 994–1004.

[13] M. Uno, K. Seto, M. Masuda, W. Ueda, S. Takahashi, *Tetrahedron Lett.* **1985**, *26*, 1553–1556.

[14] For π-conjugated compounds incorporating 1,2-diethynyl-cyclopent-1-ene moieties, see: a) A. J. Boydston, M. Laskoski, U. H. F. Bunz, M. M. Haley, *Synlett* **2002**, 981–983; b) C. Kosinski, A. Hirsch, F. W. Heinemann, F. Hampel, *Eur. J. Org. Chem.* **2001**, 3879–3890.

[15] B. Halton, Q. Lu, P. J. Stang, *Aust. J. Chem.* **1990**, *43*, 1277–1282.

[16] A. M. Boldi, J. Anthony, C. B. Knobler, F. Diederich, *Angew. Chem.* **1992**, *104*, 1270–1273; *Angew. Chem. Int. Ed. Engl.* **1992**, *31*, 1240–1242.

[17] A. Balsamo, I. Coletta, P. Domiano, A. Guglielmotti, C. Landolfi, F. Mancini, C. Milanese, E. Orlandini, S. Rapposelli, M. Pinza, B. Macchia, *Eur. J. Med. Chem.* **2002**, *37*, 391–398.

[18] K. Miwa, T. Aoyama, T. Shioiri, *Synlett* **1994**, 107–108.

[19] M. Ballester, J. Riera, *Spectrochim. Acta Part A* **1967**, *23*, 1533–1539.

[20] Transition moments were calculated at the TD-PBE1PBE/6-311+G(d,p)//B3LYP/6–31G(d) level of theory. However, TD-DFT calculations using various functionals all erroneously predicted the optical transition energies for most of the chromophores under study.

[21] a) C. Reichardt, *Solvents and Solvent Effects in Organic Chemistry*, 3rd ed., Wiley-VCH, Weinheim, **2003**; b) J. Catalán, H. Hopf, *Eur. J. Org. Chem.* **2004**, 4694–4702.

[22] F. Ammar, J. M. Savéant, *J. Electroanal. Chem. Interfacial Electrochem.* **1973**, *47*, 115–125.

[23] Gaussian 09, Revision A.1, M. J. Frisch, G. W. Trucks, H. B. Schlegel, G. E. Scuseria, M. A. Robb, J. R. Cheeseman, G. Scalmani, V. Barone, B. Mennucci, G. A. Petersson, H. Nakatsuji, M. Caricato, X. Li, H. P. Hratchian, A. F. Izmaylov, J. Bloino, G. Zheng, J. L. Sonnenberg, M. Hada, M. Ehara, K. Toyota, R. Fukuda, J. Hasegawa, M. Ishida, T. Nakajima, Y. Honda, O. Kitao, H. Nakai, T. Vreven, J. A. Montgomery, Jr., J. E. Peralta, F. Ogliaro, M. Bearpark, J. J. Heyd, E. Brothers, K. N. Kudin, V. N. Staroverov, R. Kobayashi, J. Normand, K. Raghavachari, A. Rendell, J. C. Burant, S. S. Iyengar, J. Tomasi, M. Cossi, N. Rega, J. M. Millam, M. Klene, J. E. Knox, J. B. Cross, V. Bakken, C. Adamo, J. Jaramillo, R. Gomperts, R. E. Stratmann, O. Yazyev, A. J. Austin, R. Cammi, C. Pomelli, J. W. Ochterski, R. L. Martin, K. Morokuma, V. G. Zakrzewski, G. A. Voth, P. Salvador, J. J. Dannenberg, S. Dapprich, A. D. Daniels, Ö. Farkas, J. B. Foresman, J. V. Ortiz, J. Cioslowski, D. J. Fox, Gaussian, Inc., Wallingford CT, **2009**.

[24] C. Dehu, F. Meyers, J.-L. Brédas, *J. Am. Chem. Soc.* **1993**, *115*, 6198–6206.

[25] a) M. Gholami, M. N. Chaur, M. Wilde, M. J. Ferguson, R. McDonald, L. Echegoyen, R. R. Tykwinski, *Chem. Commun.* **2009**, 3038–3040; b) G. Chen, L. Wang, D. W. Thompson, Y. Zhao, *Org. Lett.* **2008**, *10*, 657–660.

[26] a) A. Julg, Ph. François, *Theor. Chim. Acta* **1967**, *8*, 249–259; b) C. W. Bird, *Tetrahedron* **1985**, *41*, 1409–1414.

[27] H. S. Blanchette, S. C. Brand, H. Naruse, T. J. R. Weakley, M. M. Haley, *Tetrahedron* **2000**, *56*, 9581–9588.

[28] After heating **19a** in cyclohexa-1,4-diene at reflux for 1 week, a tiny mass peak at $m/z = 496.2849$ (relative intensity 7.38%, $[M+4]^+$) was observed by analyzing the crude mixture with high resolution MALDI-MS. This peak was not found by the same analysis of **19a** (see the Supporting Information).

[29] a) H. Fallah-Bagher-Shaidaei, C. S. Wannere, C. Corminboeuf, R. Puchta, P. von R. Schleyer, *Org. Lett.* **2006**, *8*, 863–866; b) P. von R. Schleyer, M. Manoharan, Z.-X. Wang, B. Kiran, H. Jiao, R. Puchta, N. J. R. v. E. Hommes, *Org. Lett.* **2001**, *3*, 2465–2468; c) P. von R. Schleyer, C. Maerker, A. Dransfeld, H. Jiao, N. J. R. v. E. Hommes, *J. Am. Chem. Soc.* **1996**, *118*, 6317–6318; d) Z. Chen, C. S. Wannere, C. Corminboeuf, R. Puchta, P. von R. Schleyer, *Chem. Rev.* **2005**, *105*, 3842–3888.

[30] S. M. Brombosz, A. J. Zucchero, P. L. McGrier, U. H. F. Bunz, *J. Org. Chem.* **2009**, *74*, 8909–8913.

[31] a) S. E. Wheeler, K. N. Houk, P. von R. Schleyer, W. D. Allen, *J. Am. Chem. Soc.* **2009**, *131*, 2547–2560; b) B. A. Hess, Jr., L. J. Schaad, *J. Am. Chem. Soc.* **1983**, *105*, 7500–7505.

[32] a) L. A. Curtiss, P. C. Redfern, K. Raghavachari, V. Rassolov, J. A. Pople, *J. Chem. Phys.* **1999**, *110*, 4703–4709; b) D. Bond, *J. Org. Chem.* **2007**, *72*, 7313–7328.

[33] a) J. B. Foresman, E. Frisch, *Exploring Chemistry with Electronic Structure Method*s, 2nd ed., Gaussian, Pittsburgh, PA, **1996**, pp. 147–148 and J. B. Foresman, E. Frisch, *Exploring Chemistry with Electronic Structure Method*s, 2nd ed., Gaussian, Pittsburgh, PA, **1996**, pp. 157–158; b) D. C. Young, *Computational Chemistry*, Wiley-Interscience, New York, **2001**, pp. 137–141.

[34] S. M. Bachrach, *Computational Organic Chemistry*, Wiley-Interscience, New York, **2007**, pp. 103–106.

[35] a) Z. Otwinowski, W. Minor, *Meth. Enzymol.* **1997**, *276*, 307–326; b) A. Altomare, M. C. Burla, M. Camalli, G. L. Cascarano, C. Giacovazzo, A. Guagliardi, A. G. G. Moliterni, G. Polidori, R. Spagna, *J. Appl. Crystallogr.* **1999**, *32*, 115; c) SHELXL97, Program for the Refinement of Crystal Structures, G. M. Sheldrick, University of Göttingen (Germany), **1997**.

Received: April 21, 2010
Published online: July 20, 2010

